

## PHOTOMETRIC SEPARATION OF STELLAR PROPERTIES USING SDSS FILTERS

DAWN D. LENZ,<sup>1</sup> HEIDI JO NEWBERG,<sup>2,3</sup> ROBERT ROSNER,<sup>1</sup> GORDON T. RICHARDS,<sup>1,2</sup> AND CHRIS STOUGHTON<sup>2,3</sup>

*Received 1997 December 15; accepted 1998 July 20*

### ABSTRACT

Using synthetic photometry of Kurucz model spectra, we explore the colors of stars as a function of temperature, metallicity, and surface gravity with Sloan Digital Sky Survey (SDSS) filters,  $u'g'r'i'z'$ . The synthetic colors show qualitative agreement with the few published observations in these filters. We find that the locus of synthetic stars is basically two-dimensional for  $4500 < T < 8000$  K, which precludes simultaneous color separation of the three basic stellar characteristics we consider. Colors including  $u'$  contain the most information about normal stellar properties; measurements in this filter are also important for selecting white dwarfs. We identify two different subsets of the locus in which the loci separate by either metallicity or surface gravity. For  $0.5 < g' - r' < 0.8$  (corresponding roughly to G stars), the locus separates by metallicity; for photometric error of a few percent, we estimate metallicity to within  $\sim 0.5$  dex in this range. In the range  $-0.15 < g' - r' < 0.00$  (corresponding roughly to A stars), the locus shows separation by surface gravity. In both cases, we show that it is advantageous to use more than two colors when determining stellar properties by color. Strategic observations in SDSS filters are required to resolve the source of a  $\sim 5\%$  discrepancy between synthetic colors of Gunn-Stryker stars, Kurucz models, and external determinations of the metallicities and surface gravities. The synthetic star colors can be used to investigate the properties of any normal star and to construct analytic expressions for the photometric prediction of stellar properties in special cases.

*Subject headings:* galaxies: photometry — surveys

### 1. INTRODUCTION

The Sloan Digital Sky Survey (SDSS) is designed to obtain high-precision photometry and spectroscopy for one-fourth of the sky to a limiting magnitude of  $V \approx 20$  (the galaxy redshift sample will be somewhat brighter than this), with a goal of mapping the universe in redshift (Gunn & Knapp 1993; Kent 1994; Gunn 1995). A survey of such depth and coverage will produce data for unprecedented numbers of a variety of objects; in particular, there will be high-quality photometric data for perhaps  $10^8$  stars and  $10^6$  quasar candidates (Gunn & Knapp 1993; Kent 1994).

The photometric system for the survey uses five broad-band filters,  $u'$ ,  $g'$ ,  $r'$ ,  $i'$ , and  $z'$ , covering 3000–11500 Å (Fig. 1). The SDSS will use the photometric data to select galaxy and quasar candidates and will then obtain spectra for those candidates. The SDSS photometric system differs from previous standard systems, as outlined in § 2.

Since the SDSS is expected to produce a large amount of data on a nonstandard photometric system, it is desirable to characterize the system in advance of the actual survey. For example, synthetic photometry can be used to gain insight into the properties of the photometric system, to estimate how the colors of objects are affected by variations in the intrinsic attributes of the objects and how those variations compare with expected photometric errors, and to estimate the regions of color space different types of objects occupy. The last issue is particularly important for the SDSS because one would like to characterize the overlap in color space of, e.g., the stellar and quasar loci, to maximize the number of quasar spectra obtained. Richards et al. (1997,

hereafter R97) discuss some of the overlap observed in their photometry, which uses SDSS filters. Synthetic photometry plays a key role in identifying potentially interesting or unusual objects and is vital to the efficient analysis of the amount of data the SDSS will produce.

We will apply the notation  $u'g'r'i'z'$  to our calculated colors, with the caveat that the calibration of the SDSS system is in progress and the comparison of our calculations to SDSS data in principle requires transformation of our colors into the final calibrated SDSS system colors (in any case, no simulation can exactly reproduce or replace observation). These simulations mimic the final SDSS system to the extent that the description in Fukugita et al. (1996, hereafter F96) reflects the actual characteristics of the system.

The purpose of this paper is twofold. We first present synthetic colors on the SDSS system for several sets of stellar spectra; this synthetic photometry can aid in the identifications of objects found in the SDSS photometric survey. Then, we show how synthetic photometry from Kurucz model spectra can be used to determine the characteristics of ordinary stars. In § 2, we describe the SDSS photometric system and the differences between this system and other photometric systems. In § 3, we describe the spectra and method for our photometry synthesis, using the stellar spectrophotometric atlas of Gunn & Stryker (Gunn & Stryker 1983, hereafter GS), white dwarf spectra (Greenstein & Liebert 1990), and stellar model atmosphere spectra (Kurucz 1991). In § 4, we compare our synthetic colors with data taken using  $u'g'r'i'z'$  filters. We present the results of our photometric metallicity separation analysis for G stars in § 5; in § 6, we discuss the photometric separation of low-gravity A stars. Section 7 summarizes our work and conclusions.

### 2. THE SDSS PHOTOMETRIC SYSTEM

F96 provides the detailed definition of the SDSS photometric system; the following is a brief description of the

<sup>1</sup> Department of Astronomy and Astrophysics, University of Chicago, 5640 South Ellis Avenue, Chicago, IL 60637; lenz@oddjob.uchicago.edu, rrosner@oddjob.uchicago.edu, richards@oddjob.uchicago.edu.

<sup>2</sup> Fermi National Accelerator Laboratory, Kirk Road and Pine Street, Batavia, IL 60510.

<sup>3</sup> heidi@fnal.gov, stoughto@fnal.gov; work supported by the US Department of Energy under contract DE-ACO2-76CH03000.

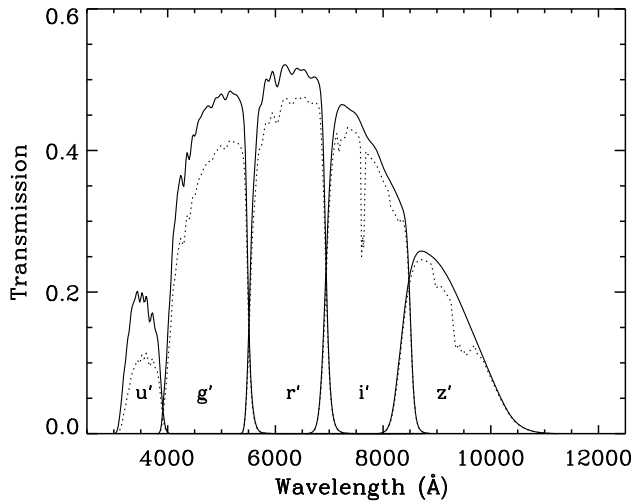


FIG. 1.—Transmission curves for the Monitor Telescope  $u'g'r'i'z'$  filters (Fukugita et al. 1996). Dotted curves are for 1.2 air masses; solid curves are without atmosphere.

system. The  $u'$ ,  $g'$ ,  $r'$ ,  $i'$ , and  $z'$  filters have effective wavelengths of 3500 Å, 4800 Å, 6200 Å, 7600 Å, and 9000 Å, respectively (Fig. 1). Magnitudes are  $AB$  magnitudes as defined by Oke & Gunn (1983, hereafter OG): the monochromatic  $AB$  magnitude is

$$AB_v = -2.5 \log f_v - 48.6, \quad (1)$$

where  $f_v$  has units of  $\text{ergs cm}^{-2} \text{s}^{-1} \text{Hz}^{-1}$ . The formal definition of the system is such that a flat spectrum (constant  $f_v$ ) has  $AB = V$ . The constant, 48.6, in the above definition provides for conversion from  $AB$  magnitude to absolute flux. The formally defined zero point of the  $AB$  system is such that a flat spectrum has all colors equal to 0. This is a physically meaningful definition because the ratios of constant- $f_v$  fluxes in different bandpasses are unity; the system definition introduces no artificial zero point.

The SDSS filters differ from the “standard”  $UBVRI$  filters (which we will take to be those discussed by Bessell 1990) in several ways. Figure 2 shows the SDSS passbands and Bessell’s  $UBVRI$  passbands. While the  $u'$  and  $U$  filters resemble each other somewhat, none of the other “standard” filters are very similar to any of the SDSS filters. The SDSS system covers a wider wavelength range

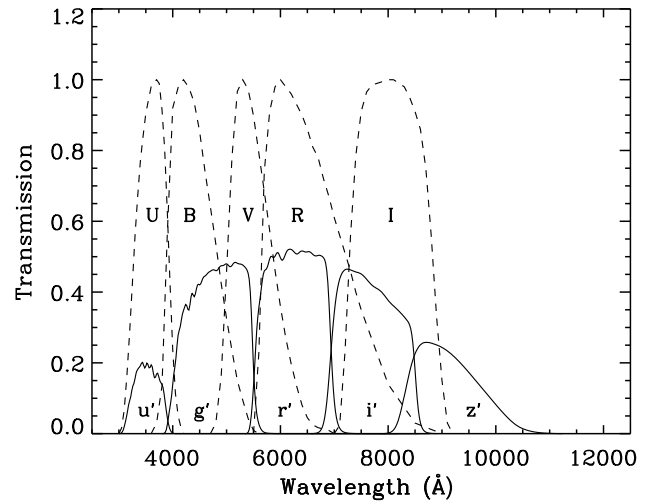


FIG. 2.—Transmission curves for the Monitor Telescope  $u'g'r'i'z'$  filters without atmosphere (solid curves; Fukugita et al. 1996) and the standard  $UBVRI$  filters (dashed curves; Bessell 1990). The  $UBVRI$  transmission curves are arbitrarily normalized to a peak transmission of 1.

(3000–11500 Å) than the standard system range (3000–9200 Å). Unlike the standard  $UBVRI$  passbands, the SDSS passbands overlap relatively little, which makes the SDSS photometry a more clearly defined diagnostic of spectral features. We refer the reader to F96 for transformations between the  $u'g'r'i'z'$  and  $UBVRI$  systems.

The  $u'g'r'i'z'$  data will be calibrated using low-metallicity F subdwarfs as secondary spectrophotometric standards. These stars are desirable standards because they are reasonably bright for modern large telescopes and have fairly flat spectra with few features (OG). See OG and F96 for a description of the standards and calibration procedure and F96 for discussion of the calibration of the SDSS system.

### 3. SYNTHETIC COLORS

We have calculated synthetic colors on the SDSS system for several sets of real and simulated stellar spectra, as summarized in Table 1:

1. The Gunn-Stryker spectrophotometric atlas (GS) provides spectra covering 3130–10800 Å for stars spanning the

TABLE 1  
LIST OF TABLES

Table	Objects
2	Spectrophotometric atlas stars of Gunn & Stryker 1983
3	White dwarfs (Greenstein & Liebert 1990)
Simulated Spectra (Kurucz 1991)	
4	Stars, $\log g \in \{4.0, 4.5\}$ , $T_{\text{eff}} = 3500\text{--}40,000$ K, $[M/H] = 0.0^a$ (“dwarfs”)
5	Stars, $\log g \in \{4.0, 4.5\}$ , $T_{\text{eff}} = 3500\text{--}35,000$ K, $[M/H] = +1.0$ (“dwarfs”)
6	Stars, $\log g \in \{4.0, 4.5\}$ , $T_{\text{eff}} = 3500\text{--}40,000$ K, $[M/H] = -1.0$ (“dwarfs”)
7	Stars, $\log g \in \{4.0, 4.5\}$ , $T_{\text{eff}} = 3500\text{--}40,000$ K, $[M/H] = -2.0$ (“dwarfs”)
8	Stars, $\log g \in \{4.0, 4.5\}$ , $T_{\text{eff}} = 4250\text{--}40,000$ K, $[M/H] = -5.0$ (“dwarfs”)
9	Stars, $\log g \in \{2.5, 3.0\}$ , $T_{\text{eff}} = 3500\text{--}26,000$ K, $[M/H] = 0.0$ (“giants”)
10	Stars, $\log g \in \{2.5, 3.0\}$ , $T_{\text{eff}} = 3500\text{--}21,000$ K, $[M/H] = +1.0$ (“giants”)
11	Stars, $\log g \in \{2.5, 3.0\}$ , $T_{\text{eff}} = 3500\text{--}26,000$ K, $[M/H] = -1.0$ (“giants”)
12	Stars, $\log g \in \{2.5, 3.0\}$ , $T_{\text{eff}} = 3500\text{--}26,000$ K, $[M/H] = -2.0$ (“giants”)
13	Stars, $\log g \in \{2.5, 3.0\}$ , $T_{\text{eff}} = 3500\text{--}26,000$ K, $[M/H] = -5.0$ (“giants”)
14	Stars, $\log g \in \{1.0, 1.5, 2.0\}$ , $T_{\text{eff}} = 4000\text{--}7000$ K, $[M/H] = -1.0$ (“horizontal-branch stars”)
15	Stars, $\log g = 5.0$ , $T_{\text{eff}} = 20,000\text{--}50,000$ K, $[M/H] = 0.0$ (“OB subdwarfs”)

<sup>a</sup>  $[M/H] \equiv \log [(M/H)_{\text{model}}/(M/H)_{\odot}]$ , where  $(M/H)$  denotes metallicity relative to hydrogen.

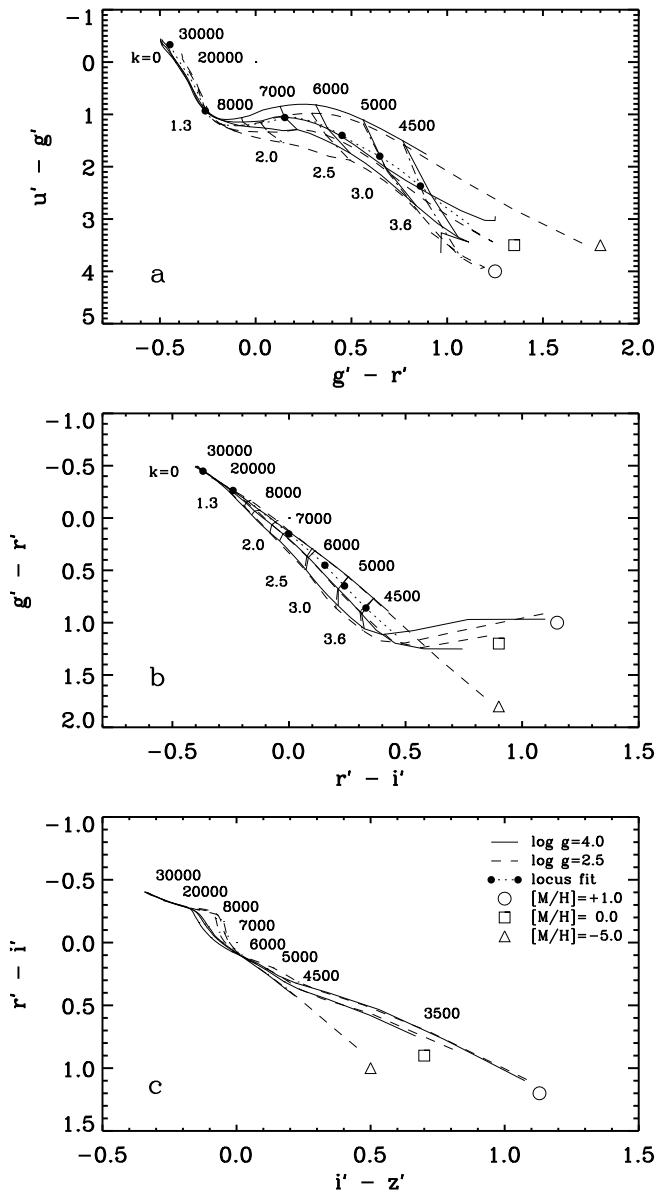


FIG. 3.—Variation in the position of the stellar locus due to temperature, surface gravity, and metallicity in (a)  $u' - g'$  vs.  $g' - r'$ , (b)  $g' - r'$  vs.  $r' - i'$ , and (c)  $r' - i'$  vs.  $i' - z'$ . Solid curves indicate Kurucz models (Kurucz 1991) with  $\log g = 4.0$ ; dashed curves indicate Kurucz models with  $\log g = 2.5$ . Three metallicities are shown, resulting in three pairs of solid/dashed curves labeled with a circle for  $[M/H] = +1.0$ , a square for  $[M/H] = 0.0$ , and a triangle for  $[M/H] = -5.0$ . Values of  $T$  are marked along the locus; solid lines indicate isotherms for the  $\log g = 4.0$  models, and dot-dashed lines indicate isotherms for the  $\log g = 2.5$  models. The dotted line is the locus fit (§ 5.1); the values of principal component  $k$  at the points corresponding to the cross-sectional  $k$  ranges shown in Fig. 7 are labeled and marked with large dots.

H-R diagram. Thirteen of the GS stars are missing data in a wavelength bin of width  $\approx 300 \text{ \AA}$  centered on  $\lambda \approx 8000 \text{ \AA}$ ; we omit these stars from our sample.

2. White dwarf spectra covering 3571–8300  $\text{\AA}$  are found in Greenstein & Liebert (1990); we extrapolate to cover the  $u'g'r'i'z'$  wavelength range using linear fits to the flux values at the shortest three given wavelengths (for the blue end) and to the flux values at the longest three given wavelengths (for the red end). While the use of spectra with complete wavelength coverage would be preferable, we nevertheless consider the resulting approximations to the positions of

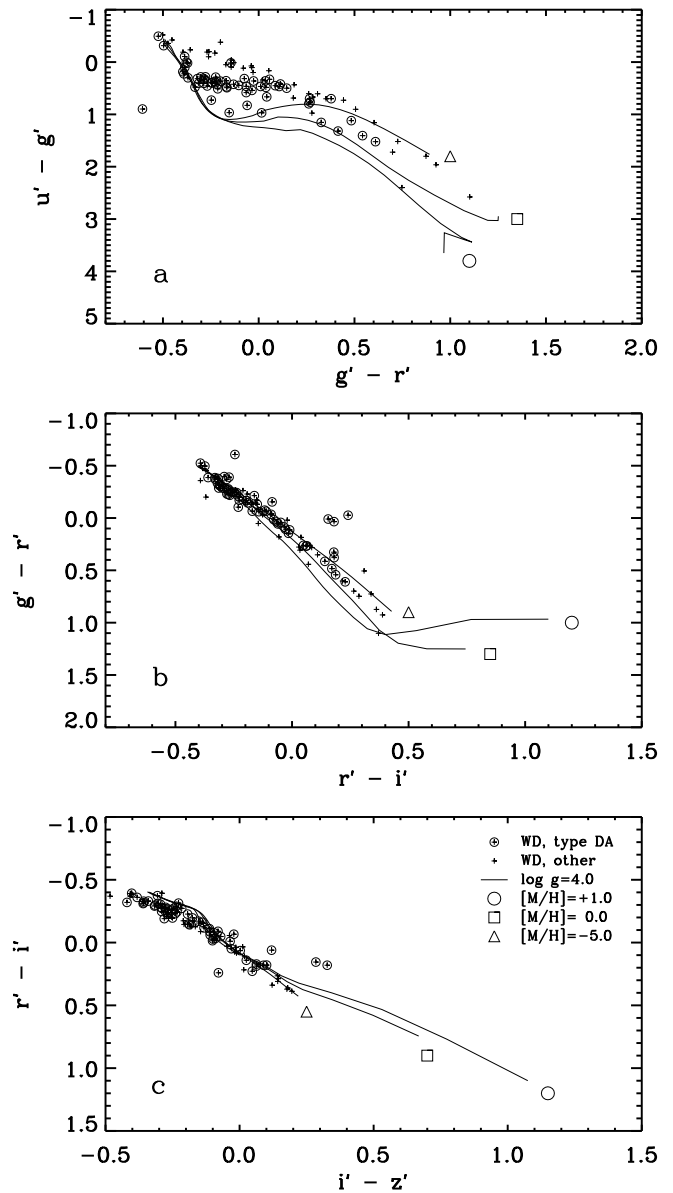


FIG. 4.—Location of white dwarfs (plus signs; Greenstein & Liebert 1990) relative to Kurucz models with  $\log g = 4.0$  and  $[M/H] = +1.0, 0.0, -5.0$  (solid curves labeled as in Fig. 3; Kurucz 1991). White dwarfs designated DA in the Greenstein & Liebert atlas are circled.

white dwarfs in color space valuable for estimating the amount of expected overlap of white dwarfs and normal stars in color space. Such overlap must be considered when investigating photometric separations in color space of the type we discuss in §§ 5 and 6 below.

3. Simulated stellar spectra are provided by the model stellar atmospheres of Kurucz (1991), covering a wide range of effective temperatures, surface gravities, and metallicities. Here, we synthesize colors for atmospheres with  $T_{\text{eff}}$  and  $\log g$  characteristic of main-sequence (dwarf) and giant stars with  $[M/H] = 0, +1, -1, -2, \text{ and } -5$ , where  $[M/H]$  denotes the metallicity relative to solar:

$$[M/H] \equiv \log [(M/H)_{\text{model}} / (M/H)_{\odot}] ; \quad (2)$$

$(M/H)$  denotes metallicity relative to hydrogen. We also synthesize colors for model spectra corresponding to horizontal-branch stars and OB subdwarfs.

TABLE 2  
SYNTHESIZED  $u'g'r'i'z'$  COLORS FOR THE GUNN-STRYKER STELLAR ATLAS

Star	Type	$u' - g'$	$g' - r'$	$r' - i'$	$i' - z'$
9 Sgr .....	O5	-0.4807	-0.5639	-0.3989	-0.2855
9 Sge .....	O8F	-0.4369	-0.5392	-0.4216	-0.3269
HR 8023 .....	O6	-0.4019	-0.5466	-0.4072	-0.3431
-1 935 .....	B1 V	-0.2565	-0.4751	-0.3620	-0.2623
60 Cyg .....	B1 V	-0.2052	-0.5083	-0.3858	-0.2985
102 Her .....	B2 V	-0.1145	-0.4791	-0.3933	-0.2963
$\eta$ Hya .....	B3 V	0.0447	-0.4195	-0.3255	-0.2223
$i$ Her .....	B3 V	0.0714	-0.4341	-0.3423	-0.2447
HR 7899 .....	B4 V	0.0887	-0.4461	-0.3498	-0.2515
38 Oph .....	A1 V	0.2729	-0.3745	-0.3096	-0.2088
HR 7174 .....	B6 V	0.4969	-0.3304	-0.2853	-0.1840
9 Vul .....	B7 V	0.5026	-0.3289	-0.2643	-0.1613
HD 189689 .....	B9 V	0.5617	-0.3068	-0.2600	-0.1280
$\theta$ Vir .....	A0 V	0.9790	-0.2533	-0.2225	-0.1205
$\nu$ Cap .....	B9 V	0.8832	-0.2590	-0.2161	-0.1021
HR 6169 .....	A2 V	1.0182	-0.2463	-0.2304	-0.1583
HD 190849A .....	A1 V	0.9620	-0.2488	-0.2151	-0.1243
69 Her .....	A2 V	1.0155	-0.2413	-0.2225	-0.1270
HD 190849B .....	A3 V	1.0510	-0.2024	-0.1974	-0.1136
58 Aql .....	A0 V	1.0547	-0.1742	-0.1844	-0.0739
78 Her .....	B9 V	1.0741	-0.1945	-0.1848	-0.1115
HR 6570 .....	A7 V	1.1581	-0.1584	-0.1904	-0.1318
HD 187754 .....	A2 V	1.2430	-0.1163	-0.1286	-0.0540
$\theta^1$ Ser .....	A5 V	1.1306	-0.1032	-0.1390	-0.0953
Praesepe 276 .....	...	1.2238	-0.0473	-0.1518	-0.0547
Praesepe 114 .....	...	1.1664	-0.0395	-0.1128	-0.0732
Praesepe 154 .....	...	1.1351	-0.0153	-0.0832	-0.0740
HD 190192 .....	A5 V	1.1502	0.0013	-0.0701	-0.0590
Praesepe 226 .....	...	1.1276	0.0522	-0.0328	-0.0607
Praesepe 37 .....	...	1.1088	0.0977	-0.0406	-0.0465
HD 191177 .....	F4 V	1.1785	0.1160	-0.0198	-0.0618
Praesepe 332 .....	...	1.0586	0.1933	-0.0002	-0.0166
BD +293891 .....	F6 V	1.1026	0.2064	0.0404	-0.0488
Praesepe 222 .....	...	1.0906	0.2174	0.0463	-0.0014
HD 35296 .....	F8 V	1.1193	0.3048	0.0735	0.0231
HD 148816 .....	F9 V	0.9831	0.3406	0.1116	0.0298
HD 155675 .....	F8 V	1.0683	0.3282	0.1230	0.0166
Praesepe 418 .....	...	1.1805	0.3345	0.0735	0.0128
HD 122693 .....	F8 V	1.2358	0.3467	0.0966	-0.0261
HD 154417 .....	F8 V	1.1709	0.3540	0.0944	-0.0061
Hyad 2 .....	...	1.2886	0.3856	0.0909	0.0239
HD 154760 .....	G2 V	1.2734	0.3865	0.1285	0.0231
HD 139777A .....	K0 V	1.2919	0.4361	0.1381	0.0214
HD 136274 .....	G8 V	1.5195	0.4926	0.1711	0.0265
HYAD 26 .....	...	1.5372	0.5038	0.1319	0.0546
HD 150205 .....	G5 V	1.5028	0.4912	0.1658	0.0510
Hyad 21 .....	...	1.6981	0.5451	0.1636	0.0752
+02 3001 .....	G8 V	1.6281	0.6197	0.2160	0.0759
Hyad 183 .....	...	1.9875	0.7079	0.2135	0.1316
HD 190470 .....	K3 V	2.0313	0.6999	0.2245	0.1008
HD 154712 .....	K4 V	2.2264	0.8254	0.2901	0.1451
Hyad 185 .....	...	2.2837	0.9170	0.3613	0.1888
+38 2457 .....	K8 V	2.4454	0.9289	0.3221	0.1348
Hyad 173 .....	...	2.6264	1.0804	0.4151	0.2422
GL 40 .....	M0 V	2.6485	1.1869	0.5150	0.2592
Hyad 189 .....	...	2.7606	1.1980	0.5304	0.2670
HD 151288 .....	K7 V	2.7246	1.2219	0.5650	0.2531
HD 157881 .....	K7 V	2.7529	1.2146	0.5816	0.2864
HD 132683 .....	M0 V	2.7564	1.2529	0.6159	0.2540
GL 15A .....	M0 V	2.7902	1.4056	0.9429	0.4277
GL 49 .....	M2 V	2.7670	1.3563	0.9599	0.4434
GL 109 .....	M4 V	2.8687	1.3709	1.2489	0.5682
GL 15B .....	M6 V	3.1937	1.5201	1.5139	0.6697
GL 83.1 .....	M8 V	3.1577	1.5271	1.7723	0.8039
GL 65 .....	M5 V	2.9529	1.5728	2.2560	1.0712
HR 7567 .....	B1 IV	-0.1459	-0.5016	-0.3974	-0.2952
HR 7591 .....	B2 III	-0.1307	-0.4757	-0.3640	-0.2731
20 Aql .....	B3 IV	0.2144	-0.4008	-0.3076	-0.2245
HR 7467 .....	B3 III	0.1761	-0.4177	-0.3396	-0.2365
$i$ Lyr .....	B7 IV	0.3502	-0.3619	-0.3079	-0.1603
HR 7346 .....	B7 III	0.4977	-0.3511	-0.2708	-0.1957
59 Her .....	A3 III	1.0347	-0.2961	-0.2450	-0.1252

TABLE 2—Continued

Star	Type	$u' - g'$	$g' - r'$	$r' - i'$	$i' - z'$
HR 6642	A0 IV	0.8936	-0.2989	-0.2556	-0.1600
11 Sge	B9 IV	0.8609	-0.2653	-0.2690	-0.1160
60 Her	A3 IV	1.1148	-0.1660	-0.1719	-0.1077
HD 192285	A4 IV	1.1348	-0.1279	-0.1449	-0.0822
$\alpha$ Oph	A5 III	1.1474	-0.0796	-0.1440	-0.0797
HD 165475B	A5 IV	1.2581	-0.0135	-0.1217	-0.0705
$\zeta$ Ser	F0 IV	1.2022	0.0061	-0.0631	-0.0569
HD 5132	F0 IV	1.1289	0.0881	-0.0753	-0.0548
HD 508	A9 IV	1.2355	0.0960	-0.0488	-0.0300
HD 210875	F0 IV	1.2694	0.0756	-0.0432	-0.0425
$\rho$ Cap	F2 IV	1.1052	0.1341	0.0011	-0.0187
HD 7331	F7 IV	1.1260	0.2172	0.0163	-0.0248
BD + 630013	F5 IV	1.1007	0.2289	0.0204	-0.0127
HD 13391	G2 IV	1.2200	0.3839	0.0734	-0.0039
HD 154962	G8 IV	1.4744	0.4287	0.1354	0.0401
HD 192344	G4 IV	1.4779	0.4165	0.1351	0.0462
HR 6516	G6 IV	1.4871	0.4271	0.1081	0.0155
HR 7670	G6 IV	1.6009	0.4546	0.1095	0.0176
HD 128428	G3 IV	1.6414	0.4989	0.1533	0.0393
31 Aql	G8 IV	1.6267	0.5282	0.1433	0.0001
-02 4018	G5 IV	1.7526	0.6150	0.1859	0.0735
M67 F143?	...	1.7977	0.6108	0.2002	0.0657
HD 11004	G5 IV	1.6891	0.6785	0.2440	0.1455
HD 173399A	G5 IV	1.8016	0.5780	0.2349	0.1113
HD 56176	G7 IV	1.8309	0.6400	0.2365	0.1399
HD 227693	G5 IV	1.9539	0.6396	0.2201	0.1274
Praesepe 212	...	2.0653	0.6782	0.1995	0.1359
$\theta^1$ Tau	G8 III	2.1162	0.6701	0.2299	0.1202
HD 170527	G5 IV	2.0322	0.6821	0.2604	0.1180
HD 136366	K0 III	2.1908	0.6934	0.2115	0.1852
HD 191615	G8 IV	2.1373	0.7436	0.2656	0.1572
HD 124679	K0 III	2.1523	0.6971	0.2516	0.1080
HD 131111	K0 III	2.2028	0.7236	0.3084	0.1465
HD 113493	K0 III	2.3106	0.7425	0.2537	0.0915
HD 4744	G8 IV	2.1322	0.8062	0.3064	0.1651
HD 7010	K0 IV	2.1672	0.7995	0.2808	0.1523
46 LMi	K0 III	2.3185	0.7760	0.2779	0.1558
91 Aqr	K0 III	2.4179	0.7835	0.2734	0.1226
M67 F141	...	2.4411	0.7780	0.2553	0.1261
HR 8924A	K3 III	2.5586	0.7847	0.2193	0.1510
HD 140301	K0 IV	2.4713	0.7687	0.2917	0.1561
HD 95272	K0 III	2.4261	0.7988	0.2966	0.1747
HD 72184	K2 III	2.5670	0.8043	0.2606	0.1681
HD 119425	K2 III	2.4812	0.7942	0.2733	0.1435
HD 106760	K1 III	2.5223	0.8352	0.3035	0.1528
$\psi$ UMa	K1 III	2.5817	0.8421	0.2994	0.1769
$\phi$ Ser	K1 III	2.6338	0.8084	0.2040	0.1904
HD 136514	K3 III	2.7931	0.8609	0.2528	0.2141
$\mu$ Aql	K3 III	2.7177	0.8876	0.2815	0.1631
HR 5227	K2 III	2.7224	0.8986	0.3519	0.1214
HD 154759	K3 III	2.7784	0.9671	0.3012	0.1828
20 Cyg	K3 III	3.0990	0.9164	0.2583	0.2162
$\alpha$ Ser	K2 III	2.7153	0.8428	0.3036	0.1735
$\mu$ Leo	K2 III	2.9109	0.9317	0.3039	0.1915
M67 F170	...	3.0702	1.0125	0.3691	0.2010
18 Lib A	K2 III	2.9833	0.9190	0.3478	0.2205
+28 2165	K1 IV	3.0511	1.0383	0.4008	0.2023
NGC 188 1_69	...	2.9708	0.9992	0.3618	0.2647
+30 2344	K3 III	3.1050	1.0559	0.4158	0.2104
HD 83618	K3 III	2.9778	1.0276	0.3966	0.2387
HD 158885	K3 III	2.9427	1.0103	0.4325	0.2494
HD 148513	K4 III	3.4217	1.1062	0.3697	0.3125
M67 T626	...	3.3319	1.1640	0.4487	0.2619
M67 IV-202	...	3.5853	1.2389	0.5644	0.2866
HD 50778	K4 III	3.3603	1.1000	0.5092	0.3341
HD 62721	K5 III	3.3588	1.1731	0.5445	0.3211
HD 116870	M0 III	3.4138	1.1913	0.5982	0.3455
HD 60522	M0 III	3.5737	1.2502	0.6240	0.3713
+2 2884	K5 III	3.5501	1.2207	0.6964	0.3556
-2 3873	M0 III	3.6958	1.3473	0.9798	0.4808
HD 104216	M2 III	3.5277	1.2846	1.0005	0.4866
HD 142804	M1 III	3.9552	1.4460	0.8862	0.6270
HD 30959	M3 III	3.8238	1.4933	1.2612	0.6047

TABLE 2—Continued

Star	Type	$u' - g'$	$g' - r'$	$r' - i'$	$i' - z'$
HD 151658.....	M2 III	3.9797	1.6081	1.2657	0.6798
–2 4025.....	M2 III	3.6524	1.4707	1.4525	0.6833
–01 3097.....	M2 III	3.6774	1.4914	1.5627	0.7506
TX Dra.....	...	3.4668	1.3912	1.6528	0.7739
Z Cyg.....	M8 III	3.4818	1.4567	1.6882	0.7932
+01 3133.....	M5 III	3.2648	1.4693	1.8615	0.9387
–2 3886.....	M5 III	3.1680	1.5534	2.0137	0.9746
W Her.....	M6 III	2.0864	1.5538	2.6493	1.2675
TY Dra.....	M8	2.7613	1.8513	2.3176	1.3506
SW Vir.....	M7 III	2.4980	2.1526	2.6300	1.4449
RZ Her.....	M6 III	1.3762	2.1467	2.8639	1.7287
R Leo.....	...	1.7471	2.8456	3.1827	2.1050
AW Cyg.....	N	5.4359	2.9537	1.0151	0.6610
WZ Cas.....	N	5.6902	2.2396	0.9873	0.8065
69 Cyg.....	B0 IB	–0.3239	–0.4611	–0.4118	–0.2051
HR 7699.....	B5 IB	0.1527	–0.4138	–0.3565	–0.2217
HR 8020.....	B8 IA	0.2536	–0.1537	–0.1980	–0.1098

NOTE.—Colors were synthesized using spectra from Gunn & Stryker 1983.

The synthetic broadband  $AB$  magnitude is defined as

$$m = -2.5 \log \frac{\int f_\nu S_\nu d(\log \nu)}{\int S_\nu d(\log \nu)} - 48.6, \quad (3)$$

where  $f_\nu$  is flux per unit frequency and  $S_\nu$  is the system response (see eq. [7] of F96). The magnitude is normalized for consistency with the formal definition of the monochromatic magnitude. Note that the argument of the logarithm is proportional to the photon count: since the SDSS filters are designed for use with CCDs rather than with photographic plates, the SDSS system is defined using photon counts rather than energy flux.

The filter responses we use in our calculations are those for the SDSS Monitor Telescope with atmospheric extinction at 1.2 air masses (Fig. 1), as the Monitor Telescope will be the instrument used to make the system-defining observations (F96).

Tables 2–15 provide the synthetic colors for each of the data sets listed in Table 1. These synthetic colors are to be used with the caveat that the algorithm above is an idealization of the photometric process. Actual observations of standard stars will define the SDSS photometric system.

In Figure 3, we show how the stellar colors vary as a function of temperature, surface gravity, and metallicity in the three  $u'g'r'i'z'$  color projections. Figure 3 shows the colors for stars of two surface gravities,  $\log g = 4.0$  and  $\log g = 2.5$ , corresponding roughly to main-sequence stars and giants, respectively; and three metallicities:  $[M/H] = +1$ , 0, and  $-5$ , to span the high-metallicity to zero-metallicity range. We note that most of the surface gravity and metallicity variation appears in Figure 3a, with some metallicity separation evident in Figure 3b; Figure 3c separates surface gravities of A stars and metallicities of M stars. The bluer colors show the most metallicity separation because most of the line-blanketing from heavy elements occurs in the shorter wavelength regions. The  $u'g'r'$  wavelength region contains the Balmer jump, a stellar spectral feature sensitive to surface gravity; hence, the variation due to surface gravity is manifest primarily in the  $u' - g'$  versus  $g' - r'$  projection (Fig. 3a). We note that the metallicity width of the stellar locus in the  $UBVRI$  system (see, e.g., Mihalas & Binney 1981) is comparable to that in the  $u'g'r'i'z'$  system, so the two systems are roughly equivalent metallicity diagnos-

tics in principle, although the expected high level of precision in the SDSS system will be essential for determining metallicities using SDSS photometry. We discuss photometric metallicity separation further in § 5.

Figure 4 shows the location of white dwarfs in color space relative to Kurucz models with  $\log g = 4.0$  and  $[M/H] = +1, 0$ , and  $-5$ . Figure 4a shows the least overlap of the white dwarf and normal star loci; Figures 4b and 4c show considerable overlap. The majority of the white dwarfs can be distinguished from normal stars by their ultraviolet excess, as has been found with other filter systems (Green, Schmidt, & Liebert 1986).

Figure 5 shows the synthetic colors for the GS stars and for Kurucz models with  $\log g = 4.0$  and  $[M/H] = +1, 0$ , and  $-5$ . GS quote errors in their synthetic  $UBVRI$  and  $uvby$  photometry of  $\sim 0.02$ – $0.04$  mag, so most of the scatter in the synthetic photometry of GS stars is likely to be intrinsic. Most of the GS colors are consistent with the Kurucz model colors; there is only one notable outlier in Figure 5a. Some of the M stars extend to cooler temperatures than the Kurucz models currently cover, since atmospheric modeling of very cool stars is difficult (Kurucz 1979, 1991).

Comparison of Figures 3 and 5 suggests that most GS stars have approximately solar metallicities. The cooler GS stars ( $T \approx 4000$  K) show some inconsistencies with the Kurucz models. In the  $u' - g'$  versus  $g' - r'$  plot, the cool stars separate slightly more by surface gravity than expected for Kurucz models with similar metallicities. Comparison of the synthetic colors of these stars with the Kurucz model colors suggests that the metallicities of these stars are approximately solar. In the  $r' - i'$  versus  $i' - z'$  plot, the redder stars ( $i' - z' \sim 0.4$ ) are more consistent with the lower metallicity models; however, the few red stars in this region with measured metallicities are nearly solar (Cayrel de Strobel et al. 1997). Resolution of such discrepancies requires careful examination of the metallicity measurement errors, the spectral calibration in the GS atlas, and the physics in the model atmospheres.

#### 4. COMPARISON WITH OBSERVATIONS

Richards et al. (1997) have obtained  $u^*g^*r^*i^*z^*$  photometry for quasars and accompanying field objects (asterisks, rather than primes, are used to denote the data since the

TABLE 3

SYNTHESIZED  $u^*g^*r^*i^*z^*$  COLORS FOR WHITE DWARF SPECTRA

Star	$u^* - g^*$	$g^* - r^*$	$r^* - i^*$	$i^* - z^*$
0009-058.....	0.5836	-0.0655	-0.1705	-0.1530
0032-175.....	0.4641	-0.0652	-0.1109	-0.1124
0038+555.....	0.0110	-0.1307	-0.1738	-0.2099
0038+730.....	-0.0376	-0.1433	-0.1560	-0.1530
0038-226.....	1.1582	0.6023	0.2167	0.0156
0046+051.....	0.9757	0.2776	0.0292	-0.0470
0052+226.....	0.3157	-0.0753	-0.1175	-0.1325
0102+210A.....	1.5212	0.6098	0.2280	0.0473
0102+210B.....	1.5184	0.7259	0.3390	0.1214
0107-192.....	0.4039	-0.3125	-0.3124	-0.3041
0112+104.....	-0.1894	-0.3955	-0.3276	-0.3612
0115+159.....	0.1056	-0.0364	-0.1268	-0.1811
0126+422.....	-0.1057	-0.3868	-0.3600	-0.3821
0143+216.....	0.3614	-0.0268	0.2405	-0.0788
0148+641.....	0.6646	0.0419	-0.0483	-0.0704
0155+069.....	0.0180	-0.3714	-0.3296	-0.3577
0213+427.....	1.4061	0.5421	0.1871	0.0629
0231-054.....	0.2889	-0.2247	-0.2377	-0.2675
0236+744.....	0.5415	-0.0353	-0.0898	-0.0805
0239+109.....	0.3300	0.0563	-0.0605	-0.1096
0243-026.....	0.6996	0.2656	0.0637	0.0023
0300-019.....	-0.1015	-0.2619	-0.2104	-0.2723
0302+621.....	0.4754	-0.1679	-0.1965	-0.1756
0316+345.....	0.3006	-0.3694	-0.2804	-0.2756
0339+523.....	0.8976	-0.6070	-0.2449	-0.2334
0348+339.....	0.3710	-0.2299	-0.2793	-0.2916
0354+463.....	0.3598	0.0346	0.1802	0.3269
0407+179.....	0.3949	-0.2473	-0.2583	-0.2528
0408-041.....	0.3303	-0.2868	-0.3143	-0.2276
0426+588.....	0.4342	0.1848	0.0383	-0.0140
0501+527.....	-0.4939	-0.5243	-0.3930	-0.4023
0501+527.....	-0.3565	-0.4741	-0.3841	-0.4022
0548-001.....	0.7294	0.4425	0.0702	-0.0141
0552-041.....	2.3996	0.7477	0.2870	0.1446
0553+053.....	1.1194	0.4834	0.1708	0.0630
0743+442.....	0.3245	-0.2832	-0.2894	-0.2360
1610+166.....	0.4064	-0.2866	-0.2985	-0.3153
1624+477.....	0.4833	0.0374	-0.0665	-0.0214
1625+093.....	0.7980	0.2615	0.0487	-0.0307
1633+572.....	0.7013	0.3514	0.1093	0.0185
1636+160.....	0.3954	-0.2253	-0.2731	-0.2456
1637+335.....	0.8277	-0.0605	-0.1418	-0.1869
1639+537.....	0.4674	0.1067	-0.0283	-0.0986
1641+387.....	0.3165	-0.3201	-0.3107	-0.3595
1645+325.....	-0.2333	-0.3576	-0.3930	-0.2897
1704+481B.....	0.9660	-0.1542	-0.0854	-0.1104
1705+481A.....	0.2246	-0.3906	-0.2700	-0.2774
1705+030.....	0.6874	0.1807	-0.0563	-0.0378
1710+683.....	0.7649	0.2682	0.0603	0.1194
1713+332.....	0.0012	-0.3779	-0.3174	-0.3576
1716+020.....	0.4296	-0.2176	-0.2669	-0.2669
1728+560.....	-0.1984	-0.2603	-0.2899	-0.2893
1748+708.....	0.9028	0.5056	0.3092	0.1422
1811+327A.....	0.4991	0.1459	-0.0151	-0.1008
1811+327B.....	1.1537	0.3263	0.1792	0.1009
1818+126.....	1.3188	0.4142	0.1408	0.0251
1822+410.....	-0.1909	-0.2700	-0.2423	-0.2341
1824+040.....	0.7278	-0.2474	-0.2475	-0.2907
1826-045.....	0.9701	0.0153	-0.0783	-0.0958
1827-106.....	0.4569	-0.2686	-0.2719	-0.2891
1829+547.....	0.6061	0.3072	0.0339	0.0116
1855+338.....	0.3571	-0.1703	-0.2263	-0.2691
1900+706.....	0.0143	-0.1452	-0.1908	-0.2809
1917+386.....	0.6679	0.2823	0.0844	-0.0115
1917-077.....	0.0496	-0.1716	-0.1520	-0.1349
1932-136.....	0.1840	-0.3961	-0.2909	-0.3170
2002-110.....	1.8003	0.8735	0.3619	0.1797
2003+437.....	0.4001	-0.2433	-0.2375	-0.2692
2010+310.....	-0.3794	-0.2001	-0.3695	-0.4830
2010+613.....	0.4791	-0.3328	-0.3199	-0.4199
2047+372.....	0.2831	-0.3024	-0.3053	-0.2950
2048+263.....	1.7216	0.6987	0.2646	0.1410
2054-050.....	1.9635	0.9258	0.3880	0.1948

TABLE 3—Continued

Star	$u^* - g^*$	$g^* - r^*$	$r^* - i^*$	$i^* - z^*$
2058+342.....	0.0333	-0.1465	-0.2013	-0.2533
2059+316.....	0.1993	-0.0296	-0.1262	-0.1651
2107-216.....	0.7002	0.3781	0.1805	0.0897
2111+261.....	0.4509	0.0863	-0.0331	-0.0898
2111+498.....	-0.3135	-0.4965	-0.3738	-0.3062
2114+239.....	-0.4222	-0.4530	-0.3694	-0.4084
2136+229.....	0.4244	-0.1316	-0.1491	-0.1892
2139+115.....	0.2825	-0.2780	-0.2728	-0.2157
2140+207.....	0.0741	-0.0390	-0.0874	-0.1453
2147+280.....	-0.1711	-0.2291	-0.1925	-0.2650
2148+286.....	-0.5187	-0.5013	-0.3907	-0.4074
2151-015.....	0.4658	0.0097	0.1551	0.2846
2207+142.....	0.4196	0.1134	-0.0101	-0.0353
2215+386.....	0.1655	0.0525	-0.1447	-0.2074
2251-070.....	2.5778	1.1019	0.3710	0.1765
2258+406.....	0.4462	-0.1041	-0.2306	-0.2396
2307+636.....	0.1033	-0.3861	-0.3305	-0.3402
2311-068.....	0.3409	0.0203	-0.0206	-0.0926
2311+552.....	0.5111	-0.2138	-0.1618	-0.1372
2312-024.....	0.6039	0.2609	0.0759	-0.0182
2317-173.....	0.0984	-0.1439	-0.1715	-0.1742
2323+157.....	0.1163	-0.0805	-0.1443	-0.1941
2326+049.....	0.3651	-0.1998	-0.2268	-0.1937
2347+128.....	0.4900	-0.1662	-0.1960	-0.2501

NOTE.—Colors were synthesized using spectra from Greenstein & Liebert 1990.

SDSS calibration, observing conditions, and instruments will inevitably differ somewhat from those under which these data were taken). The observations were taken with the 0.6 m Monitor Telescope at Apache Point Observatory in Sunspot, NM, which will be used to take the calibration data for the SDSS data taken with the dedicated 2.5 m SDSS telescope. The data were calibrated with observations of the F subdwarfs BD +26°2606 and BD +17°4708, which are two of the fundamental standard stars that define the SDSS system (F96). Thus, the observations and the simulations are calibrated to the same system. We estimate a 10% total error in the  $u^*g^*r^*$  and  $g^*r^*i^*$  colors and 20% total error in the  $r^*i^*z^*$  colors. Note that the errors in Tables 4 and 5 of R97 are the Poisson errors for the program objects; however, the field stars used here are typically fainter than the program objects. The errors quoted above can be understood by considering the faintness of the field stars compared to the program objects and the additional errors described in Table 6 of R97. The larger errors in  $r^*i^*z^*$  are probably due to fringing and reduced throughput in the  $z$  filter.

Figure 6 shows R97's observed colors for the (mostly stellar) field objects obtained with the Monitor Telescope together with the synthetic colors for Kurucz model atmospheres with  $\log g = 4.0$ ,  $[M/H] = 0$ . Figure 6 shows that the synthetic  $u^*g^*r^*i^*z^*$  colors of the model stars are consistent with observed colors. The observed objects are generally of two types: (1) stars from the standard star fields, which were mostly equatorial and had relatively short (10–30 s) exposure times; and (2) stars from quasar fields, which were generally at high Galactic latitude and had longer (1–3 minutes) exposure times. The limiting magnitudes for the short exposure time fields were  $u^*, z^* \sim 16$  and  $g^*, r^*, i^* \sim 17.25$ , while the limits for the longer exposures are somewhat fainter. Thus, the sample of observed stars is fairly heterogeneous in metallicity, color, and magnitude.

TABLE 4

SYNTHESIZED  $u'g'r'i'z'$  COLORS FOR STELLAR MODEL ATMOSPHERES WITH  $[M/H] = 0.0$ ,  $\log g \in \{4.0, 4.5\}$ 

$T_{\text{eff}}$ (K)	$\log g$	$u' - g'$	$g' - r'$	$r' - i'$	$i' - z'$
3500	4.0	2.9474	1.2513	0.7444	0.6680
	4.5	2.9443	1.3039	0.7188	0.6247
3750	4.0	3.0289	1.2498	0.5781	0.4969
	4.5	2.9310	1.2776	0.5707	0.4578
4000	4.0	3.0257	1.1961	0.4550	0.3457
	4.5	2.9149	1.2159	0.4654	0.3344
4250	4.0	2.8393	1.0716	0.3744	0.2358
	4.5	2.8041	1.0964	0.3791	0.2384
4500	4.0	2.5400	0.9164	0.3117	0.1776
	4.5	2.5453	0.9408	0.3132	0.1764
4750	4.0	2.2599	0.7827	0.2573	0.1390
	4.5	2.2676	0.7981	0.2586	0.1364
5000	4.0	2.0126	0.6775	0.2112	0.1060
	4.5	2.0211	0.6846	0.2121	0.1036
5250	4.0	1.7838	0.5908	0.1734	0.0750
	4.5	1.7929	0.5936	0.1735	0.0737
5500	4.0	1.5791	0.5136	0.1407	0.0467
	4.5	1.5837	0.5154	0.1406	0.0461
5750	4.0	1.4087	0.4419	0.1113	0.0213
	4.5	1.4044	0.4443	0.1113	0.0211
6000	4.0	1.2756	0.3763	0.0832	-0.0010
	4.5	1.2600	0.3797	0.0841	-0.0011
6250	4.0	1.1783	0.3153	0.0555	-0.0208
	4.5	1.1511	0.3200	0.0577	-0.0213
6500	4.0	1.1129	0.2578	0.0286	-0.0392
	4.5	1.0732	0.2644	0.0323	-0.0399
6750	4.0	1.0724	0.2033	0.0015	-0.0556
	4.5	1.0202	0.2122	0.0071	-0.0569
7000	4.0	1.0544	0.1511	-0.0257	-0.0707
	4.5	0.9931	0.1632	-0.0183	-0.0730
7250	4.0	1.0499	0.1007	-0.0532	-0.0845
	4.5	0.9814	0.1162	-0.0435	-0.0882
7500	4.0	1.1273	0.0268	-0.0946	-0.0996
	4.5	0.9808	0.0706	-0.0690	-0.1024
7750	4.0	1.1383	-0.0201	-0.1219	-0.1105
	4.5	1.0526	0.0061	-0.1064	-0.1191
8000	4.0	1.1459	-0.0668	-0.1474	-0.1188
	4.5	1.0649	-0.0361	-0.1316	-0.1304
8250	4.0	1.1457	-0.1132	-0.1692	-0.1255
	4.5	1.0739	-0.0777	-0.1553	-0.1404
8500	4.0	1.1309	-0.1521	-0.1884	-0.1310
	4.5	1.0752	-0.1190	-0.1757	-0.1480
8750	4.0	1.1043	-0.1827	-0.2051	-0.1365
	4.5	1.0652	-0.1555	-0.1930	-0.1539
9000	4.0	1.0689	-0.2078	-0.2187	-0.1408
	4.5	1.0442	-0.1845	-0.2084	-0.1592
9250	4.0	1.0297	-0.2289	-0.2300	-0.1451
	4.5	1.0159	-0.2077	-0.2212	-0.1642
9500	4.0	0.9880	-0.2465	-0.2395	-0.1494
	4.5	0.9839	-0.2275	-0.2319	-0.1689
9750	4.0	0.9441	-0.2612	-0.2476	-0.1536
	4.5	0.9486	-0.2444	-0.2411	-0.1730
10000	4.0	0.8988	-0.2735	-0.2546	-0.1576
	4.5	0.9106	-0.2591	-0.2490	-0.1767
10500	4.0	0.8062	-0.2923	-0.2657	-0.1658
	4.5	0.8284	-0.2821	-0.2617	-0.1836
11000	4.0	0.7175	-0.3058	-0.2744	-0.1753
	4.5	0.7457	-0.2991	-0.2716	-0.1907
11500	4.0	0.6339	-0.3161	-0.2812	-0.1853
	4.5	0.6648	-0.3117	-0.2795	-0.1982
12000	4.0	0.5572	-0.3248	-0.2868	-0.1953
	4.5	0.5891	-0.3218	-0.2859	-0.2063
12500	4.0	0.4881	-0.3325	-0.2918	-0.2047
	4.5	0.5197	-0.3303	-0.2914	-0.2145
13000	4.0	0.4265	-0.3400	-0.2964	-0.2131
	4.5	0.4566	-0.3381	-0.2962	-0.2223
14000	4.0	0.3225	-0.3539	-0.3051	-0.2277
	4.5	0.3489	-0.3522	-0.3051	-0.2359
15000	4.0	0.2381	-0.3672	-0.3133	-0.2397
	4.5	0.2610	-0.3654	-0.3130	-0.2473
16000	4.0	0.1673	-0.3799	-0.3210	-0.2501
	4.5	0.1879	-0.3778	-0.3206	-0.2569

TABLE 4—Continued

$T_{\text{eff}}$ (K)	$\log g$	$u' - g'$	$g' - r'$	$r' - i'$	$i' - z'$
17000	4.0	0.1050	-0.3917	-0.3285	-0.2592
	4.5	0.1250	-0.3895	-0.3279	-0.2653
18000	4.0	0.0493	-0.4029	-0.3356	-0.2674
	4.5	0.0693	-0.4006	-0.3347	-0.2729
19000	4.0	-0.0015	-0.4133	-0.3424	-0.2749
	4.5	0.0189	-0.4111	-0.3413	-0.2797
20000	4.0	-0.0483	-0.4231	-0.3487	-0.2818
	4.5	-0.0274	-0.4209	-0.3475	-0.2860
21000	4.0	-0.0917	-0.4319	-0.3549	-0.2885
	4.5	-0.0701	-0.4301	-0.3536	-0.2920
22000	4.0	-0.1324	-0.4398	-0.3607	-0.2948
	4.5	-0.1096	-0.4386	-0.3593	-0.2977
23000	4.0	-0.1709	-0.4467	-0.3657	-0.3007
	4.5	-0.1468	-0.4463	-0.3648	-0.3032
24000	4.0	-0.2068	-0.4528	-0.3701	-0.3060
	4.5	-0.1820	-0.4532	-0.3697	-0.3084
25000	4.0	-0.2394	-0.4587	-0.3742	-0.3107
	4.5	-0.2150	-0.4594	-0.3741	-0.3131
26000	4.0	-0.2685	-0.4649	-0.3783	-0.3151
	4.5	-0.2454	-0.4654	-0.3783	-0.3173
27000	4.0	-0.2948	-0.4715	-0.3828	-0.3194
	4.5	-0.2729	-0.4714	-0.3823	-0.3214
28000	4.0	-0.3194	-0.4784	-0.3874	-0.3236
	4.5	-0.2980	-0.4778	-0.3866	-0.3252
29000	4.0	-0.3433	-0.4847	-0.3919	-0.3276
	4.5	-0.3216	-0.4843	-0.3909	-0.3290
30000	4.0	-0.3663	-0.4898	-0.3956	-0.3312
	4.5	-0.3441	-0.4904	-0.3951	-0.3326
31000	4.0	-0.3877	-0.4933	-0.3983	-0.3342
	4.5	-0.3656	-0.4957	-0.3987	-0.3358
32000	4.0	-0.4071	-0.4954	-0.4003	-0.3364
	4.5	-0.3858	-0.5000	-0.4017	-0.3385
33000	4.0	-0.4236	-0.4962	-0.4011	-0.3379
	4.5	-0.4043	-0.5032	-0.4041	-0.3408
34000	4.0	-0.4374	-0.4962	-0.4012	-0.3386
	4.5	-0.4205	-0.5051	-0.4058	-0.3425
35000	4.0	-0.4488	-0.4960	-0.4007	-0.3385
	4.5	-0.4345	-0.5061	-0.4067	-0.3435
37500	4.5	-0.4605	-0.5069	-0.4069	-0.3437
40000	4.5	-0.4771	-0.5095	-0.4080	-0.3438

NOTE.—Colors were synthesized using spectra from Kurucz 1991.

The outliers in Figure 6 may be nonstellar objects (such as galaxies), stars with unusual colors, or observational aberrations (such as stars contaminated with cosmic rays). Careful photometric and spectroscopic analysis of such data is required to identify all objects. One of the prerequisites of the SDSS is the determination of the probability that an object with given colors is a given type of object, in order to optimize spectroscopic fiber allocation based on photometry.

In addition to photometric errors, interstellar reddening could be a possible source of errors and discrepancies in Figure 6. The GS spectra used to synthesize the colors are dereddened, but R97's observed colors are not dereddened. The effect of reddening on  $u'g'r'i'z'$  colors must be determined observationally.

## 5. PHOTOMETRIC METALLICITY SEPARATION

### 5.1. Nonlinear Principal Component Analysis

As we will show, stellar metallicity separation analysis benefits from a more sophisticated analysis than simple examination of the color projections (Fig. 3). We note that the  $r' - i'$  versus  $i' - z'$  projection (Fig. 3c) shows little metallicity separation for all but the coolest stars and thus we will not consider it for this purpose.



TABLE 5

SYNTHESIZED  $u'g'r'i'z'$  COLORS FOR STELLAR MODEL ATMOSPHERES WITH  $[M/H] = +1.0$ ,  $\log g \in \{4.0, 4.5\}$ 

$T_{\text{eff}}$ (K)	$\log g$	$u' - g'$	$g' - r'$	$r' - i'$	$i' - z'$
3500	4.0	3.6505	0.9667	1.0994	1.0750
	4.5	3.7278	1.0437	1.0168	0.9763
3750	4.0	3.2627	0.9691	0.7684	0.7723
	4.5	3.2549	0.9756	0.7729	0.7725
4000	4.0	3.3982	1.0762	0.5329	0.5309
	4.5	3.2661	1.0559	0.5458	0.5438
4250	4.0	3.4404	1.1136	0.4001	0.3435
	4.5	3.3003	1.0988	0.4082	0.3586
4500	4.0	3.3489	1.0577	0.3230	0.2218
	4.5	3.2358	1.0591	0.3271	0.2273
4750	4.0	3.0854	0.9498	0.2636	0.1557
	4.5	3.0224	0.9582	0.2676	0.1519
5000	4.0	2.7466	0.8390	0.2112	0.1154
	4.5	2.7157	0.8445	0.2152	0.1088
5250	4.0	2.4327	0.7416	0.1673	0.0801
	4.5	2.4157	0.7431	0.1702	0.0749
5500	4.0	2.1614	0.6555	0.1320	0.0451
	4.5	2.1511	0.6552	0.1331	0.0427
5750	4.0	1.9353	0.5739	0.1016	0.0122
	4.5	1.9216	0.5740	0.1021	0.0114
6000	4.0	1.7473	0.4953	0.0732	-0.0168
	4.5	1.7270	0.4973	0.0740	-0.0172
6250	4.0	1.5935	0.4203	0.0446	-0.0414
	4.5	1.5664	0.4247	0.0464	-0.0423
6500	4.0	1.4712	0.3501	0.0159	-0.0623
	4.5	1.4365	0.3564	0.0191	-0.0641
6750	4.0	1.3606	0.2811	-0.0123	-0.0797
	4.5	1.3174	0.2900	-0.0075	-0.0828
7000	4.0	1.2920	0.2179	-0.0405	-0.0951
	4.5	1.2406	0.2309	-0.0338	-0.0995
7250	4.0	1.3106	0.1424	-0.0807	-0.1130
	4.5	1.1854	0.1737	-0.0600	-0.1144
7500	4.0	1.2774	0.0848	-0.1088	-0.1245
	4.5	1.2057	0.1072	-0.0964	-0.1333
7750	4.0	1.2545	0.0277	-0.1356	-0.1337
	4.5	1.1813	0.0550	-0.1222	-0.1451
8000	4.0	1.2374	-0.0303	-0.1602	-0.1404
	4.5	1.1640	0.0043	-0.1470	-0.1550
8250	4.0	1.2156	-0.0822	-0.1823	-0.1464
	4.5	1.1511	-0.0464	-0.1694	-0.1634
8500	4.0	1.1782	-0.1231	-0.2006	-0.1519
	4.5	1.1337	-0.0941	-0.1893	-0.1696
8750	4.0	1.1359	-0.1594	-0.2170	-0.1563
	4.5	1.1030	-0.1323	-0.2063	-0.1748
9000	4.0	1.0862	-0.1913	-0.2306	-0.1593
	4.5	1.0662	-0.1659	-0.2212	-0.1792
9250	4.0	1.0331	-0.2184	-0.2421	-0.1622
	4.5	1.0236	-0.1948	-0.2338	-0.1830
9500	4.0	0.9805	-0.2411	-0.2519	-0.1653
	4.5	0.9789	-0.2199	-0.2446	-0.1861
9750	4.0	0.9296	-0.2596	-0.2603	-0.1685
	4.5	0.9332	-0.2412	-0.2537	-0.1883
10000	4.0	0.8802	-0.2749	-0.2674	-0.1717
	4.5	0.8887	-0.2591	-0.2615	-0.1908
10500	4.0	0.7852	-0.2978	-0.2791	-0.1801
	4.5	0.8038	-0.2867	-0.2746	-0.1974
11000	4.0	0.6917	-0.3139	-0.2877	-0.1900
	4.5	0.7192	-0.3067	-0.2848	-0.2046
11500	4.0	0.6016	-0.3258	-0.2941	-0.2007
	4.5	0.6348	-0.3212	-0.2927	-0.2127
12000	4.0	0.5178	-0.3357	-0.2993	-0.2109
	4.5	0.5533	-0.3325	-0.2988	-0.2215
12500	4.0	0.4425	-0.3446	-0.3038	-0.2203
	4.5	0.4773	-0.3420	-0.3038	-0.2299
13000	4.0	0.3762	-0.3530	-0.3083	-0.2287
	4.5	0.4085	-0.3506	-0.3083	-0.2377
14000	4.0	0.2652	-0.3686	-0.3169	-0.2431
	4.5	0.2915	-0.3657	-0.3165	-0.2511
15000	4.0	0.1747	-0.3823	-0.3250	-0.2550
	4.5	0.1973	-0.3795	-0.3241	-0.2621

TABLE 5—Continued

$T_{\text{eff}}$ (K)	$\log g$	$u' - g'$	$g' - r'$	$r' - i'$	$i' - z'$
16000	4.0	0.0988	-0.3947	-0.3326	-0.2650
	4.5	0.1196	-0.3918	-0.3315	-0.2712
17000	4.0	0.0337	-0.4060	-0.3399	-0.2738
	4.5	0.0535	-0.4031	-0.3383	-0.2792
18000	4.0	-0.0230	-0.4167	-0.3471	-0.2815
	4.5	-0.0032	-0.4136	-0.3451	-0.2861
19000	4.0	-0.0739	-0.4264	-0.3540	-0.2891
	4.5	-0.0533	-0.4236	-0.3517	-0.2927
20000	4.0	-0.1211	-0.4348	-0.3606	-0.2963
	4.5	-0.0985	-0.4329	-0.3582	-0.2990
21000	4.0	-0.1659	-0.4416	-0.3664	-0.3031
	4.5	-0.1408	-0.4411	-0.3644	-0.3053
22000	4.0	-0.2083	-0.4470	-0.3708	-0.3094
	4.5	-0.1812	-0.4479	-0.3699	-0.3114
23000	4.0	-0.2471	-0.4517	-0.3744	-0.3147
	4.5	-0.2198	-0.4534	-0.3746	-0.3169
24000	4.0	-0.2810	-0.4566	-0.3777	-0.3193
	4.5	-0.2555	-0.4584	-0.3782	-0.3218
25000	4.0	-0.3100	-0.4623	-0.3816	-0.3236
	4.5	-0.2872	-0.4633	-0.3817	-0.3258
26000	4.0	-0.3353	-0.4687	-0.3863	-0.3278
	4.5	-0.3148	-0.4686	-0.3855	-0.3296
27000	4.0	-0.3583	-0.4750	-0.3913	-0.3320
	4.5	-0.3391	-0.4745	-0.3897	-0.3334
28000	4.0	-0.3798	-0.4806	-0.3960	-0.3361
	4.5	-0.3610	-0.4805	-0.3943	-0.3371
29000	4.0	-0.3996	-0.4850	-0.3997	-0.3395
	4.5	-0.3812	-0.4861	-0.3987	-0.3407
30000	4.0	-0.4175	-0.4880	-0.4023	-0.3421
	4.5	-0.4000	-0.4909	-0.4024	-0.3438
31000	4.0	-0.4330	-0.4902	-0.4037	-0.3438
	4.5	-0.4170	-0.4948	-0.4053	-0.3464
32000	4.5	-0.4322	-0.4978	-0.4073	-0.3484
33000	4.5	-0.4453	-0.5002	-0.4085	-0.3495
34000	4.5	-0.4565	-0.5023	-0.4089	-0.3500
35000	4.5	-0.4659	-0.5044	-0.4090	-0.3499

NOTE.—Colors were synthesized using spectra from Kurucz 1991.

In order to study the locus in three dimensions, we perform what amounts to a nonlinear principal component analysis on the synthetic colors of the Kurucz models given in Tables 4–15. We will use the notation of Newberg & Yanny (1997, hereafter NY97). They developed an algorithm that fits loci that are more or less one-dimensional; however, the locus of our synthetic colors looks more like a sheet (i.e., a two-dimensional surface embedded in multidimensional color space) because we have simulated stellar colors for a wide range of metallicities and because the selected grid of model temperatures, surface gravities, and metallicities is not weighted by any expected observational distribution. Therefore, we use a modified version of the NY97 algorithm: we generate the locus fit by selecting a set of  $[M/H] = -1.0$  model stellar colors from the approximate center of the distribution. For stars cooler than  $\sim 5000$  K, the  $\log g = 1.0$  curve is closest to the locus center; for stars hotter than  $\sim 7000$  K, the  $\log g = 3.0$  curve fits best. We use points from the  $\log g = 1.5, 2.0,$  and  $2.5$  models to make a smooth transition from  $T = 5000$  to  $7000$  K.

Once the locus points are chosen, a set of three mutually perpendicular unit vectors,  $\hat{k}$ ,  $\hat{l}$ , and  $\hat{m}$ , is found for each point, with  $\hat{k}$  indicating the direction of greatest variation,  $\hat{l}$  the direction of greatest variation perpendicular to  $\hat{k}$ , and  $\hat{m}$  the direction of least variation perpendicular to  $\hat{k}$ . Figure 3 shows the locus center, as defined by the adopted locus

TABLE 6

SYNTHESIZED  $u'g'r'i'z'$  COLORS FOR STELLAR MODEL ATMOSPHERES WITH  
[M/H] = -1.0,  $\log g \in \{4.0, 4.5\}$ 

$T_{\text{eff}}$ (K)	$\log g$	$u' - g'$	$g' - r'$	$r' - i'$	$i' - z'$
3500	4.0	3.1400	1.4712	0.6636	0.4310
	4.5	3.1792	1.4990	0.6696	0.4244
3750	4.0	2.8553	1.3093	0.5621	0.3295
	4.5	2.8316	1.3211	0.5650	0.3271
4000	4.0	2.6352	1.1409	0.4729	0.2656
	4.5	2.5871	1.1514	0.4787	0.2622
4250	4.0	2.3634	0.9579	0.3829	0.2135
	4.5	2.3561	0.9804	0.3949	0.2129
4500	4.0	2.0629	0.8030	0.3171	0.1703
	4.5	2.1066	0.8230	0.3185	0.1690
4750	4.0	1.7963	0.6882	0.2666	0.1345
	4.5	1.8361	0.6978	0.2668	0.1332
5000	4.0	1.5609	0.6007	0.2253	0.1029
	4.5	1.5934	0.6040	0.2248	0.1018
5250	4.0	1.3602	0.5261	0.1896	0.0747
	4.5	1.3812	0.5284	0.1893	0.0740
5500	4.0	1.2016	0.4580	0.1579	0.0499
	4.5	1.2086	0.4613	0.1580	0.0495
5750	4.0	1.0842	0.3928	0.1275	0.0279
	4.5	1.0750	0.3970	0.1286	0.0276
6000	4.0	1.0047	0.3329	0.0985	0.0076
	4.5	0.9799	0.3378	0.1006	0.0076
6250	4.0	0.9569	0.2776	0.0701	-0.0112
	4.5	0.9177	0.2837	0.0734	-0.0110
6500	4.0	0.9332	0.2264	0.0424	-0.0293
	4.5	0.8822	0.2342	0.0471	-0.0290
6750	4.0	0.9270	0.1781	0.0147	-0.0460
	4.5	0.8664	0.1879	0.0212	-0.0463
7000	4.0	0.9339	0.1310	-0.0128	-0.0617
	4.5	0.8656	0.1436	-0.0046	-0.0628
7250	4.0	0.9498	0.0850	-0.0404	-0.0759
	4.5	0.8757	0.1008	-0.0304	-0.0784
7500	4.0	0.9734	0.0384	-0.0683	-0.0887
	4.5	0.8933	0.0587	-0.0562	-0.0931
7750	4.0	1.0720	-0.0328	-0.1084	-0.1013
	4.5	0.9178	0.0163	-0.0824	-0.1066
8000	4.0	1.0960	-0.0757	-0.1351	-0.1107
	4.5	1.0074	-0.0454	-0.1182	-0.1207
8250	4.0	1.1100	-0.1180	-0.1583	-0.1174
	4.5	1.0310	-0.0838	-0.1427	-0.1313
8500	4.0	1.1107	-0.1560	-0.1779	-0.1231
	4.5	1.0461	-0.1212	-0.1649	-0.1397
8750	4.0	1.0970	-0.1851	-0.1956	-0.1288
	4.5	1.0500	-0.1562	-0.1829	-0.1462
9000	4.0	1.0726	-0.2086	-0.2104	-0.1343
	4.5	1.0417	-0.1851	-0.1987	-0.1517
9250	4.0	1.0369	-0.2274	-0.2223	-0.1389
	4.5	1.0206	-0.2068	-0.2124	-0.1575
9500	4.0	0.9956	-0.2434	-0.2321	-0.1431
	4.5	0.9925	-0.2254	-0.2240	-0.1625
9750	4.0	0.9506	-0.2565	-0.2400	-0.1477
	4.5	0.9586	-0.2410	-0.2337	-0.1673
10000	4.0	0.9045	-0.2675	-0.2467	-0.1520
	4.5	0.9201	-0.2544	-0.2417	-0.1711
10500	4.0	0.8131	-0.2844	-0.2574	-0.1595
	4.5	0.8373	-0.2754	-0.2541	-0.1777
11000	4.0	0.7310	-0.2975	-0.2659	-0.1684
	4.5	0.7583	-0.2911	-0.2638	-0.1846
11500	4.0	0.6566	-0.3082	-0.2731	-0.1777
	4.5	0.6849	-0.3037	-0.2717	-0.1917
12000	4.0	0.5884	-0.3174	-0.2795	-0.1870
	4.5	0.6169	-0.3142	-0.2786	-0.1991
12500	4.0	0.5261	-0.3259	-0.2851	-0.1960
	4.5	0.5543	-0.3234	-0.2847	-0.2068
13000	4.0	0.4692	-0.3337	-0.2904	-0.2042
	4.5	0.4966	-0.3316	-0.2902	-0.2143
14000	4.0	0.3700	-0.3483	-0.3000	-0.2191
	4.5	0.3948	-0.3466	-0.2999	-0.2281
15000	4.0	0.2865	-0.3621	-0.3089	-0.2317
	4.5	0.3090	-0.3604	-0.3087	-0.2400
16000	4.0	0.2146	-0.3751	-0.3170	-0.2427
	4.5	0.2353	-0.3734	-0.3168	-0.2501

TABLE 6—Continued

$T_{\text{eff}}$ (K)	$\log g$	$u' - g'$	$g' - r'$	$r' - i'$	$i' - z'$
17000	4.0	0.1507	-0.3870	-0.3248	-0.2524
	4.5	0.1708	-0.3853	-0.3245	-0.2592
18000	4.0	0.0926	-0.3981	-0.3320	-0.2611
	4.5	0.1128	-0.3965	-0.3315	-0.2673
19000	4.0	0.0390	-0.4082	-0.3385	-0.2690
	4.5	0.0596	-0.4069	-0.3381	-0.2746
20000	4.0	-0.0103	-0.4178	-0.3445	-0.2761
	4.5	0.0107	-0.4165	-0.3441	-0.2812
21000	4.0	-0.0554	-0.4265	-0.3502	-0.2827
	4.5	-0.0346	-0.4255	-0.3498	-0.2872
22000	4.0	-0.0965	-0.4349	-0.3557	-0.2889
	4.5	-0.0760	-0.4340	-0.3551	-0.2928
23000	4.0	-0.1344	-0.4427	-0.3609	-0.2947
	4.5	-0.1137	-0.4421	-0.3603	-0.2982
24000	4.0	-0.1697	-0.4499	-0.3657	-0.3002
	4.5	-0.1486	-0.4496	-0.3654	-0.3033
25000	4.0	-0.2025	-0.4568	-0.3702	-0.3052
	4.5	-0.1812	-0.4567	-0.3701	-0.3081
26000	4.0	-0.2330	-0.4635	-0.3747	-0.3100
	4.5	-0.2118	-0.4635	-0.3746	-0.3127
27000	4.0	-0.2614	-0.4703	-0.3791	-0.3145
	4.5	-0.2404	-0.4701	-0.3789	-0.3169
28000	4.0	-0.2885	-0.4771	-0.3836	-0.3190
	4.5	-0.2674	-0.4766	-0.3831	-0.3210
29000	4.0	-0.3150	-0.4835	-0.3880	-0.3232
	4.5	-0.2930	-0.4831	-0.3873	-0.3249
30000	4.0	-0.3411	-0.4892	-0.3914	-0.3270
	4.5	-0.3179	-0.4893	-0.3914	-0.3286
31000	4.0	-0.3659	-0.4935	-0.3939	-0.3302
	4.5	-0.3421	-0.4950	-0.3948	-0.3320
32000	4.0	-0.3887	-0.4966	-0.3955	-0.3327
	4.5	-0.3651	-0.4997	-0.3975	-0.3348
33000	4.0	-0.4086	-0.4983	-0.3962	-0.3347
	4.5	-0.3865	-0.5038	-0.3995	-0.3372
34000	4.0	-0.4253	-0.4986	-0.3960	-0.3357
	4.5	-0.4055	-0.5067	-0.4008	-0.3391
35000	4.0	-0.4391	-0.4981	-0.3949	-0.3360
	4.5	-0.4220	-0.5084	-0.4012	-0.3404
37500	4.5	-0.4528	-0.5089	-0.3993	-0.3408
40000	4.5	-0.4711	-0.5098	-0.3981	-0.3402

NOTE.—Colors were synthesized using spectra from Kurucz 1991.

points, as well as several values of  $k$  for reference;  $k$  roughly parameterizes the locus “length,” or temperature variation. The  $\hat{k}$  unit vector at a given locus point is in the direction from the closest bluer locus point to the closest redder locus point. We assume that the thin direction along the entire locus is approximately  $\hat{t} \equiv (0.125, -0.585, 0.801)$  since we know from previous studies that this will produce a reasonable result. This unit vector is not in the same direction as  $\hat{m}$ , since  $\hat{m}$  is required to be perpendicular to  $\hat{k}$ . The unit vector  $\hat{l} = \hat{t} \times \hat{k}$  lies along the wider axis of the locus cross section. The unit vector  $\hat{m} = \hat{k} \times \hat{l}$  lies along the thinner axis of the locus cross section. To assign values of  $k$ ,  $l$ , and  $m$  to a synthetic star, one first determines the locus point in multi-color space closest to the colors for that star;  $l$  and  $m$  are the distances from this closest point in the  $\hat{l}$  and  $\hat{m}$  directions, respectively, and  $k$  is the distance in the  $\hat{k}$  direction between the model colors and the closest locus point plus the value of  $k$  corresponding to that locus point.

Figure 7 shows the variation in the cross section of the locus as a function of the distance along it, parameterized by  $k$ . Stars with  $1.3 < k < 2.0$  ( $T \sim 8000$  K) are primarily separated by surface gravity (Fig. 7b), and stars with  $2.5 < k < 3.6$  ( $T \sim 5000$  K) are primarily separated by metallicity (Figs. 7d and 7e). In between (Fig. 7c), the width

TABLE 7

SYNTHESIZED  $u'g'r'i'z'$  COLORS FOR STELLAR MODEL ATMOSPHERES WITH  
[M/H] = -2.0, log  $g \in \{4.0, 4.5\}$ 

$T_{\text{eff}}$ (K)	log $g$	$u' - g'$	$g' - r'$	$r' - i'$	$i' - z'$
3500	4.0	2.5005	1.1435	0.4390	0.2471
	4.5	2.9684	1.5213	0.6628	0.3806
3750	4.0	2.6573	1.2592	0.5604	0.3130
	4.5	2.6179	1.2818	0.5604	0.3129
4000	4.0	2.3584	1.0626	0.4744	0.2604
	4.5	2.3267	1.0766	0.4763	0.2593
4250	4.0	2.0777	0.8976	0.3960	0.2138
	4.5	2.0651	0.9121	0.4017	0.2133
4500	4.0	1.8065	0.7636	0.3284	0.1721
	4.5	1.8097	0.7777	0.3356	0.1724
4750	4.0	1.5385	0.6648	0.2824	0.1374
	4.5	1.5561	0.6709	0.2843	0.1373
5000	4.0	1.3149	0.5804	0.2410	0.1075
	4.5	1.3377	0.5853	0.2421	0.1068
5250	4.0	1.1413	0.5046	0.2042	0.0813
	4.5	1.1590	0.5104	0.2048	0.0806
5500	4.0	1.0225	0.4373	0.1701	0.0577
	4.5	1.0139	0.4390	0.1705	0.0573
5750	4.0	0.9394	0.3746	0.1374	0.0357
	4.5	0.9214	0.3798	0.1395	0.0359
6000	4.0	0.8884	0.3181	0.1064	0.0153
	4.5	0.8566	0.3240	0.1095	0.0157
6250	4.0	0.8621	0.2666	0.0775	-0.0043
	4.5	0.8186	0.2732	0.0813	-0.0035
6500	4.0	0.8550	0.2183	0.0492	-0.0226
	4.5	0.8006	0.2265	0.0542	-0.0218
6750	4.0	0.8620	0.1719	0.0215	-0.0399
	4.5	0.7985	0.1823	0.0281	-0.0396
7000	4.0	0.8796	0.1264	-0.0059	-0.0561
	4.5	0.8085	0.1397	0.0021	-0.0564
7250	4.0	0.9048	0.0814	-0.0333	-0.0712
	4.5	0.8280	0.0979	-0.0236	-0.0725
7500	4.0	0.9396	0.0350	-0.0624	-0.0843
	4.5	0.8533	0.0570	-0.0493	-0.0877
7750	4.0	1.0416	-0.0342	-0.1015	-0.0965
	4.5	0.8834	0.0160	-0.0754	-0.1019
8000	4.0	1.0736	-0.0761	-0.1289	-0.1065
	4.5	0.9807	-0.0457	-0.1115	-0.1157
8250	4.0	1.0954	-0.1175	-0.1534	-0.1140
	4.5	1.0123	-0.0837	-0.1371	-0.1271
8500	4.0	1.1015	-0.1550	-0.1734	-0.1198
	4.5	1.0332	-0.1202	-0.1600	-0.1362
8750	4.0	1.0917	-0.1839	-0.1913	-0.1258
	4.5	1.0417	-0.1541	-0.1786	-0.1430
9000	4.0	1.0693	-0.2069	-0.2066	-0.1314
	4.5	1.0380	-0.1836	-0.1947	-0.1487
9250	4.0	1.0357	-0.2256	-0.2189	-0.1360
	4.5	1.0193	-0.2052	-0.2090	-0.1544
9500	4.0	0.9955	-0.2410	-0.2288	-0.1403
	4.5	0.9928	-0.2234	-0.2209	-0.1597
9750	4.0	0.9530	-0.2537	-0.2368	-0.1449
	4.5	0.9606	-0.2387	-0.2306	-0.1648
10000	4.0	0.9100	-0.2642	-0.2436	-0.1492
	4.5	0.9243	-0.2516	-0.2387	-0.1686
10500	4.0	0.8247	-0.2810	-0.2544	-0.1571
	4.5	0.8478	-0.2722	-0.2514	-0.1755
11000	4.0	0.7453	-0.2941	-0.2630	-0.1657
	4.5	0.7724	-0.2880	-0.2612	-0.1825
11500	4.0	0.6729	-0.3051	-0.2704	-0.1746
	4.5	0.7005	-0.3007	-0.2693	-0.1893
12000	4.0	0.6070	-0.3147	-0.2769	-0.1837
	4.5	0.6340	-0.3114	-0.2763	-0.1965
12500	4.0	0.5467	-0.3234	-0.2829	-0.1924
	4.5	0.5729	-0.3208	-0.2825	-0.2040
13000	4.0	0.4916	-0.3316	-0.2885	-0.2006
	4.5	0.5167	-0.3293	-0.2882	-0.2114
14000	4.0	0.3944	-0.3470	-0.2985	-0.2155
	4.5	0.4173	-0.3450	-0.2984	-0.2250
15000	4.0	0.3110	-0.3611	-0.3077	-0.2285
	4.5	0.3323	-0.3593	-0.3076	-0.2372
16000	4.0	0.2378	-0.3742	-0.3162	-0.2397
	4.5	0.2581	-0.3724	-0.3161	-0.2477

TABLE 7—Continued

$T_{\text{eff}}$ (K)	log $g$	$u' - g'$	$g' - r'$	$r' - i'$	$i' - z'$
17000	4.0	0.1725	-0.3861	-0.3241	-0.2498
	4.5	0.1922	-0.3846	-0.3239	-0.2570
18000	4.0	0.1128	-0.3971	-0.3313	-0.2589
	4.5	0.1327	-0.3960	-0.3310	-0.2654
19000	4.0	0.0578	-0.4072	-0.3378	-0.2670
	4.5	0.0780	-0.4062	-0.3376	-0.2731
20000	4.0	0.0071	-0.4164	-0.3437	-0.2743
	4.5	0.0275	-0.4157	-0.3436	-0.2799
21000	4.0	-0.0391	-0.4251	-0.3492	-0.2809
	4.5	-0.0192	-0.4244	-0.3491	-0.2860
22000	4.0	-0.0808	-0.4334	-0.3544	-0.2871
	4.5	-0.0616	-0.4328	-0.3544	-0.2916
23000	4.0	-0.1186	-0.4415	-0.3596	-0.2928
	4.5	-0.0999	-0.4408	-0.3594	-0.2969
24000	4.0	-0.1533	-0.4492	-0.3646	-0.2983
	4.5	-0.1349	-0.4485	-0.3644	-0.3020
25000	4.0	-0.1858	-0.4566	-0.3695	-0.3036
	4.5	-0.1672	-0.4560	-0.3692	-0.3068
26000	4.0	-0.2165	-0.4638	-0.3742	-0.3085
	4.5	-0.1976	-0.4632	-0.3738	-0.3115
27000	4.0	-0.2458	-0.4708	-0.3787	-0.3132
	4.5	-0.2265	-0.4701	-0.3782	-0.3159
28000	4.0	-0.2745	-0.4775	-0.3832	-0.3179
	4.5	-0.2542	-0.4768	-0.3827	-0.3201
29000	4.0	-0.3028	-0.4837	-0.3873	-0.3221
	4.5	-0.2811	-0.4833	-0.3868	-0.3241
30000	4.0	-0.3310	-0.4891	-0.3907	-0.3259
	4.5	-0.3075	-0.4893	-0.3907	-0.3278
31000	4.0	-0.3580	-0.4931	-0.3931	-0.3291
	4.5	-0.3334	-0.4946	-0.3941	-0.3311
32000	4.0	-0.3828	-0.4960	-0.3946	-0.3318
	4.5	-0.3581	-0.4994	-0.3966	-0.3340
33000	4.0	-0.3810	-0.5032	-0.3986	-0.3364
34000	4.0	-0.4013	-0.5060	-0.3999	-0.3382
35000	4.0	-0.4187	-0.5073	-0.4003	-0.3395
37500	4.0	-0.4505	-0.5068	-0.3980	-0.3395
40000	4.0	-0.4687	-0.5070	-0.3964	-0.3387

NOTE.—Colors were synthesized using spectra from Kurucz 1991.

of the distribution is due to a combination of surface gravity and metallicity. These results apply to dereddened stars or stars for which there is very little reddening.

These results partially corroborate the NY97 results for observations of bright stars in  $WBVR$  filters. In particular, the Kurucz model colors predict that the stellar locus for a set of stars with a variety of temperatures, surface gravities, and metallicities will be a ribbon in  $u' - g', g' - r', r' - i'$  multicolor space. The locus is quite thin for stars hotter than  $\sim 4500$  K, while the very red end of the locus, which is populated by M stars, can broaden considerably, depending on the stellar parameters (Fig. 7f). The width of the locus of G and K stars is primarily determined by the metallicities of the individual stars in the sample. We further note that the width of the locus for A stars is primarily determined by surface gravity. We suspect that the tight distribution in Figure 8 of NY97, which shows [M/H] versus cross-locus distance for a sample of F and G dwarfs, was obtained in part because the dwarfs exhibit a narrow range of surface gravities. NY97 probably could not note this from their sample, since hotter stars were almost exclusively dwarfs and cooler stars were almost exclusively giants; thus, the broadening of the locus of bright  $WBVR$  stars by surface gravity is substantially reduced.

### 5.2. Metallicity Separation for G Stars

As Figures 3 and 7 show, most of the cross-locus

TABLE 8

SYNTHESIZED  $u'g'r'i'z'$  COLORS FOR STELLAR MODEL ATMOSPHERES WITH  $[M/H] = -5.0, \log g \in \{4.0, 4.5\}$ 

$T_{\text{eff}}$ (K)	$\log g$	$u' - g'$	$g' - r'$	$r' - i'$	$i' - z'$
4250	4.0	1.7640	0.8921	0.4270	0.2190
4500	4.0	1.5001	0.7671	0.3624	0.1793
4750	4.0	1.2772	0.6553	0.3046	0.1455
	4.5	1.2946	0.6674	0.3078	0.1448
5000	4.0	1.1064	0.5615	0.2549	0.1155
	4.5	1.1156	0.5700	0.2577	0.1149
5250	4.0	0.9875	0.4871	0.2134	0.0884
	4.5	0.9872	0.4935	0.2154	0.0882
5500	4.0	0.9072	0.4240	0.1768	0.0637
	4.5	0.8953	0.4291	0.1790	0.0637
5750	4.0	0.8519	0.3664	0.1429	0.0411
	4.5	0.8297	0.3714	0.1456	0.0415
6000	4.0	0.8186	0.3137	0.1111	0.0200
	4.5	0.7855	0.3190	0.1146	0.0207
6250	4.0	0.8057	0.2647	0.0817	0.0001
	4.5	0.7622	0.2720	0.0858	0.0009
6500	4.0	0.8080	0.2180	0.0531	-0.0188
	4.5	0.7540	0.2261	0.0584	-0.0177
6750	4.0	0.8229	0.1723	0.0253	-0.0365
	4.5	0.7595	0.1830	0.0318	-0.0359
7000	4.0	0.8473	0.1275	-0.0022	-0.0530
	4.5	0.7759	0.1410	0.0056	-0.0530
7250	4.0	0.8782	0.0833	-0.0295	-0.0682
	4.5	0.8007	0.0998	-0.0201	-0.0693
7500	4.0	0.9159	0.0378	-0.0582	-0.0820
	4.5	0.8311	0.0588	-0.0459	-0.0848
7750	4.0	1.0253	-0.0324	-0.0976	-0.0941
	4.5	0.8654	0.0184	-0.0720	-0.0995
8000	4.0	1.0624	-0.0740	-0.1256	-0.1045
	4.5	0.9667	-0.0434	-0.1079	-0.1133
8250	4.0	1.0879	-0.1148	-0.1507	-0.1125
	4.5	1.0031	-0.0815	-0.1339	-0.1251
8500	4.0	1.0977	-0.1528	-0.1711	-0.1184
	4.5	1.0278	-0.1181	-0.1575	-0.1344
8750	4.0	1.0904	-0.1821	-0.1893	-0.1244
	4.5	1.0385	-0.1515	-0.1765	-0.1417
9000	4.0	1.0698	-0.2052	-0.2047	-0.1301
	4.5	1.0375	-0.1818	-0.1927	-0.1473
9250	4.0	1.0382	-0.2239	-0.2172	-0.1348
	4.5	1.0205	-0.2034	-0.2072	-0.1533
9500	4.0	1.0001	-0.2393	-0.2273	-0.1392
	4.5	0.9958	-0.2219	-0.2193	-0.1586
9750	4.0	0.9595	-0.2518	-0.2356	-0.1439
	4.5	0.9652	-0.2370	-0.2293	-0.1637
10000	4.0	0.9174	-0.2625	-0.2424	-0.1481
	4.5	0.9306	-0.2500	-0.2376	-0.1677
10500	4.0	0.8330	-0.2793	-0.2533	-0.1561
	4.5	0.8559	-0.2707	-0.2504	-0.1747
11000	4.0	0.7541	-0.2926	-0.2619	-0.1645
	4.5	0.7810	-0.2866	-0.2603	-0.1817
11500	4.0	0.6826	-0.3038	-0.2693	-0.1731
	4.5	0.7096	-0.2995	-0.2684	-0.1884
12000	4.0	0.6180	-0.3137	-0.2760	-0.1820
	4.5	0.6438	-0.3104	-0.2754	-0.1955
12500	4.0	0.5592	-0.3227	-0.2822	-0.1906
	4.5	0.5834	-0.3200	-0.2817	-0.2028
13000	4.0	0.5051	-0.3312	-0.2879	-0.1988
	4.5	0.5283	-0.3288	-0.2876	-0.2101
14000	4.0	0.4089	-0.3468	-0.2984	-0.2138
	4.5	0.4301	-0.3448	-0.2982	-0.2237
15000	4.0	0.3251	-0.3611	-0.3078	-0.2269
	4.5	0.3451	-0.3592	-0.3076	-0.2360
16000	4.0	0.2508	-0.3741	-0.3163	-0.2385
	4.5	0.2701	-0.3725	-0.3161	-0.2468
17000	4.0	0.1841	-0.3860	-0.3242	-0.2487
	4.5	0.2030	-0.3846	-0.3240	-0.2562
18000	4.0	0.1233	-0.3968	-0.3313	-0.2579
	4.5	0.1425	-0.3958	-0.3310	-0.2648
19000	4.0	0.0675	-0.4067	-0.3377	-0.2662
	4.5	0.0868	-0.4058	-0.3377	-0.2724
20000	4.0	0.0163	-0.4158	-0.3435	-0.2735
	4.5	0.0357	-0.4152	-0.3436	-0.2794

TABLE 8—Continued

$T_{\text{eff}}$ (K)	$\log g$	$u' - g'$	$g' - r'$	$r' - i'$	$i' - z'$
21000	4.0	-0.0302	-0.4244	-0.3489	-0.2801
	4.5	-0.0114	-0.4239	-0.3490	-0.2855
22000	4.0	-0.0719	-0.4328	-0.3541	-0.2863
	4.5	-0.0540	-0.4322	-0.3541	-0.2911
23000	4.0	-0.1093	-0.4410	-0.3593	-0.2921
	4.5	-0.0924	-0.4402	-0.3591	-0.2965
24000	4.0	-0.1437	-0.4490	-0.3644	-0.2976
	4.5	-0.1272	-0.4481	-0.3641	-0.3014
25000	4.0	-0.1759	-0.4569	-0.3695	-0.3029
	4.5	-0.1593	-0.4558	-0.3690	-0.3062
26000	4.0	-0.2065	-0.4645	-0.3745	-0.3080
	4.5	-0.1894	-0.4633	-0.3738	-0.3110
27000	4.0	-0.2363	-0.4718	-0.3793	-0.3130
	4.5	-0.2183	-0.4705	-0.3785	-0.3156
28000	4.0	-0.2662	-0.4786	-0.3839	-0.3176
	4.5	-0.2465	-0.4774	-0.3830	-0.3200
29000	4.0	-0.2965	-0.4845	-0.3879	-0.3221
	4.5	-0.2745	-0.4839	-0.3872	-0.3241
30000	4.0	-0.3267	-0.4892	-0.3909	-0.3260
	4.5	-0.3024	-0.4897	-0.3910	-0.3279
31000	4.0	-0.3553	-0.4929	-0.3930	-0.3290
	4.5	-0.3298	-0.4947	-0.3943	-0.3312
32000	4.0	-0.3810	-0.4955	-0.3943	-0.3315
	4.5	-0.3558	-0.4992	-0.3966	-0.3339
33000	4.0	-0.4028	-0.4967	-0.3949	-0.3333
	4.5	-0.3795	-0.5028	-0.3983	-0.3361
34000	4.0	-0.4207	-0.4965	-0.3945	-0.3344
	4.5	-0.4002	-0.5052	-0.3995	-0.3380
35000	4.0	-0.4352	-0.4953	-0.3932	-0.3345
	4.5	-0.4177	-0.5065	-0.3998	-0.3390
37500	4.5	-0.4495	-0.5055	-0.3974	-0.3390
40000	4.5	-0.4675	-0.5056	-0.3956	-0.3381

NOTE.—Colors were synthesized using spectra from Kurucz 1991.

variation is due to metallicity in the range  $R \equiv 0.5 < g' - r' < 0.8$  ( $2.5 < k < 3.6$ ), corresponding roughly to G stars. For  $g' - r' < 0.5$  and  $g' - r' > 0.8$ , the stellar colors are either insensitive to metallicity or the effects of metallicity on the colors cannot be separated from the effects of surface gravity.

We focus on  $l$  as the component showing the greatest sensitivity to metallicity. We calculate  $l$  in the range  $R$  using the formula  $l \cong (r - r_0) \cdot \hat{l}$ , where  $r \equiv (u' - g', g' - r', r' - i')$ ,  $r_0 = (1.799, 0.648, 0.238)$  is a point near the center of the locus region corresponding to  $R$ , and  $\hat{l} = (-0.436, 0.693, 0.574)$  is the direction of  $\hat{l}$  at that point. In Figure 8 we show metallicity as a function of  $l$  for  $[M/H] = +1.0$  to  $-5$  in region  $R$ . The width of the distribution may reflect error in the Kurucz models as well as intrinsic spread in the stellar locus; modeling error, however, is likely to induce mostly systematic errors and therefore is unlikely to affect significantly the relative colors (Kurucz 1979). Stars with  $l \lesssim -0.05$  have solar or higher metallicity. Stars with very low metallicities occupy the range  $l \gtrsim 0.19$ . In the range  $-0.05 < l < 0.19$ , the synthetic colors of the Kurucz models suggest that we can determine the metallicity to  $\pm 0.5$  dex for the theoretical stellar “sample” we have selected. The width depends on the distribution of surface gravities and will thus be a function of observational sample. For example, a bright sample might contain only giants at G, and a faint sample might contain essentially all dwarfs; if the sample contained only stars with  $4.0 \leq \log g \leq 4.5$ , the width of the distribution would be roughly half of that shown in Figure 8.

TABLE 9

SYNTHESIZED  $u'g'r'i'z'$  COLORS FOR STELLAR MODEL ATMOSPHERES WITH  $[M/H] = 0.0$ ,  $\log g \in \{2.5, 3.0\}$ 

$T_{\text{eff}}$ (K)	$\log g$	$u' - g'$	$g' - r'$	$r' - i'$	$i' - z'$
3500	2.5	3.1998	1.1275	0.8498	0.8066
	3.0	3.0517	1.1240	0.8511	0.8059
3750	2.5	3.4376	1.2388	0.5679	0.5039
	3.0	3.2768	1.2161	0.5767	0.5227
4000	2.5	3.3290	1.1813	0.4472	0.3199
	3.0	3.2091	1.1787	0.4479	0.3290
4250	2.5	3.0040	1.0321	0.3706	0.2355
	3.0	2.9237	1.0382	0.3727	0.2329
4500	2.5	2.6629	0.8921	0.3045	0.1894
	3.0	2.5944	0.8919	0.3077	0.1840
4750	2.5	2.3630	0.7814	0.2504	0.1505
	3.0	2.3078	0.7751	0.2529	0.1463
5000	2.5	2.0896	0.6877	0.2086	0.1124
	3.0	2.0478	0.6804	0.2092	0.1106
5250	2.5	1.8496	0.6004	0.1736	0.0772
	3.0	1.8121	0.5953	0.1735	0.0767
5500	2.5	1.6536	0.5184	0.1417	0.0473
	3.0	1.6138	0.5154	0.1416	0.0471
5750	2.5	1.5029	0.4409	0.1090	0.0229
	3.0	1.4590	0.4408	0.1106	0.0219
6000	2.5	1.3938	0.3668	0.0767	0.0028
	3.0	1.3448	0.3707	0.0795	0.0005
6250	2.5	1.3215	0.2967	0.0443	-0.0140
	3.0	1.2668	0.3037	0.0487	-0.0177
6500	2.5	1.2801	0.2290	0.0113	-0.0276
	3.0	1.2188	0.2405	0.0181	-0.0334
6750	2.5	1.3407	0.1277	-0.0401	-0.0372
	3.0	1.1945	0.1792	-0.0130	-0.0469
7000	2.5	1.3349	0.0640	-0.0738	-0.0445
	3.0	1.2674	0.0868	-0.0616	-0.0580
7250	2.5	1.3322	-0.0012	-0.1057	-0.0494
	3.0	1.2702	0.0295	-0.0931	-0.0665
7500	2.5	1.3224	-0.0637	-0.1346	-0.0532
	3.0	1.2740	-0.0294	-0.1229	-0.0730
7750	2.5	1.2938	-0.1116	-0.1602	-0.0568
	3.0	1.2675	-0.0858	-0.1487	-0.0777
8000	2.5	1.2510	-0.1525	-0.1825	-0.0600
	3.0	1.2445	-0.1304	-0.1724	-0.0821
8250	2.5	1.1966	-0.1864	-0.2008	-0.0640
	3.0	1.2072	-0.1672	-0.1926	-0.0864
8500	2.5	1.1343	-0.2132	-0.2152	-0.0684
	3.0	1.1577	-0.1979	-0.2088	-0.0898
8750	2.5	1.0682	-0.2327	-0.2263	-0.0735
	3.0	1.1026	-0.2221	-0.2219	-0.0940
9000	2.5	1.0046	-0.2475	-0.2351	-0.0803
	3.0	1.0472	-0.2413	-0.2326	-0.0991
9250	2.5	0.9420	-0.2580	-0.2422	-0.0879
	3.0	0.9907	-0.2563	-0.2412	-0.1044
9500	2.5	0.8802	-0.2658	-0.2476	-0.0964
	3.0	0.9339	-0.2680	-0.2483	-0.1101
9750	2.5	0.8205	-0.2716	-0.2520	-0.1057
	3.0	0.8778	-0.2769	-0.2541	-0.1167
10000	2.5	0.7636	-0.2766	-0.2557	-0.1153
	3.0	0.8238	-0.2841	-0.2591	-0.1238
10500	2.5	0.6576	-0.2851	-0.2621	-0.1339
	3.0	0.7213	-0.2952	-0.2669	-0.1390
11000	2.5	0.5629	-0.2930	-0.2674	-0.1506
	3.0	0.6274	-0.3041	-0.2730	-0.1541
11500	2.5	0.4801	-0.3007	-0.2726	-0.1651
	3.0	0.5430	-0.3120	-0.2783	-0.1678
12000	2.5	0.4087	-0.3087	-0.2776	-0.1774
	3.0	0.4688	-0.3197	-0.2833	-0.1798
12500	2.5	0.3468	-0.3167	-0.2828	-0.1881
	3.0	0.4042	-0.3274	-0.2882	-0.1903
13000	2.5	0.2919	-0.3246	-0.2878	-0.1976
	3.0	0.3476	-0.3351	-0.2930	-0.1996
14000	2.5	0.1962	-0.3393	-0.2977	-0.2142
	3.0	0.2513	-0.3497	-0.3023	-0.2156
15000	2.5	0.1134	-0.3530	-0.3069	-0.2285
	3.0	0.1708	-0.3638	-0.3112	-0.2291
16000	2.5	0.0382	-0.3650	-0.3155	-0.2412
	3.0	0.1000	-0.3767	-0.3198	-0.2409

TABLE 9—Continued

$T_{\text{eff}}$ (K)	$\log g$	$u' - g'$	$g' - r'$	$r' - i'$	$i' - z'$
17000	2.5	-0.0317	-0.3751	-0.3233	-0.2527
	3.0	0.0361	-0.3886	-0.3278	-0.2516
18000	2.5	-0.0984	-0.3824	-0.3297	-0.2634
	3.0	-0.0227	-0.3994	-0.3354	-0.2612
19000	2.5	-0.1633	-0.3864	-0.3340	-0.2732
	3.0	-0.0777	-0.4086	-0.3425	-0.2702
20000	3.0	-0.1297	-0.4160	-0.3485	-0.2786
21000	3.0	-0.1790	-0.4216	-0.3530	-0.2863
22000	3.0	-0.2239	-0.4266	-0.3565	-0.2929
23000	3.0	-0.2632	-0.4319	-0.3600	-0.2986
24000	3.0	-0.2980	-0.4379	-0.3642	-0.3038
25000	3.0	-0.3312	-0.4426	-0.3684	-0.3091
26000	3.0	-0.3646	-0.4434	-0.3703	-0.3135

NOTE.—Colors were synthesized using spectra from Kurucz 1991.

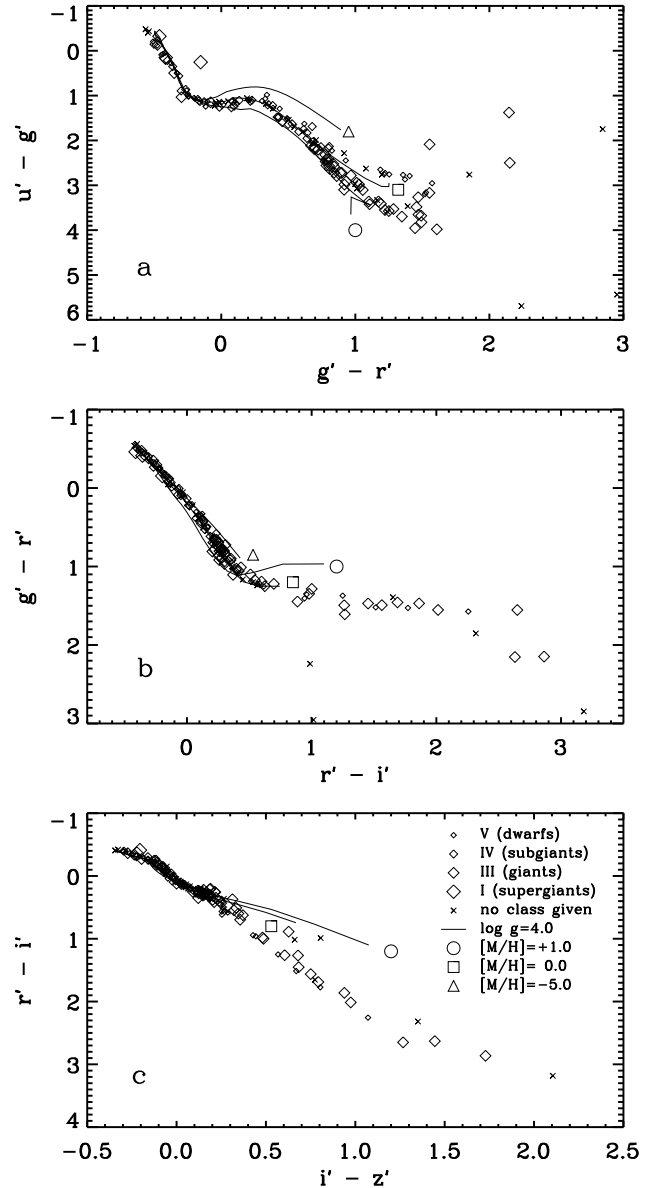
FIG. 5.—Comparison of synthetic colors for Gunn-Stryker stars (diamonds and crosses) with Kurucz model atmospheres for  $\log g = 4.0$ ,  $[M/H] = +1.0, 0.0, -5.0$  (solid curves labeled as in Fig. 3; Kurucz 1991). The size of the diamond indicates the luminosity class tabulated by GS.

TABLE 10

SYNTHESIZED  $u'g'r'i'z'$  COLORS FOR STELLAR MODEL ATMOSPHERES WITH  
[M/H] = +1.0,  $\log g \in \{2.5, 3.0\}$ 

$T_{\text{eff}}$ (K)	$\log g$	$u' - g'$	$g' - r'$	$r' - i'$	$i' - z'$
3500	2.5	3.2592	0.9155	1.0908	1.0824
	3.0	3.1933	0.8971	1.1095	1.0982
3750	2.5	3.7232	1.0887	0.7102	0.7193
	3.0	3.5242	1.0338	0.7328	0.7408
4000	2.5	3.9237	1.1948	0.4962	0.4728
	3.0	3.7296	1.1505	0.5069	0.4918
4250	2.5	3.9482	1.1725	0.3870	0.3131
	3.0	3.7643	1.1521	0.3898	0.3190
4500	2.5	3.7330	1.0713	0.3137	0.2295
	3.0	3.5968	1.0634	0.3168	0.2225
4750	2.5	3.3226	0.9593	0.2514	0.1800
	3.0	3.2352	0.9500	0.2557	0.1706
5000	2.5	2.8978	0.8582	0.2000	0.1358
	3.0	2.8400	0.8471	0.2037	0.1297
5250	2.5	2.5447	0.7640	0.1608	0.0902
	3.0	2.4988	0.7545	0.1626	0.0884
5500	2.5	2.2674	0.6714	0.1291	0.0481
	3.0	2.2223	0.6652	0.1302	0.0474
5750	2.5	2.0486	0.5792	0.0989	0.0128
	3.0	2.0005	0.5775	0.1004	0.0128
6000	2.5	1.8724	0.4909	0.0673	-0.0134
	3.0	1.8218	0.4924	0.0702	-0.0151
6250	2.5	1.8037	0.3848	0.0220	-0.0329
	3.0	1.6761	0.4116	0.0387	-0.0370
6500	2.5	1.6989	0.3023	-0.0137	-0.0476
	3.0	1.6379	0.3150	-0.0056	-0.0557
6750	2.5	1.6031	0.2208	-0.0488	-0.0580
	3.0	1.5434	0.2386	-0.0393	-0.0694
7000	2.5	1.5404	0.1426	-0.0824	-0.0649
	3.0	1.4842	0.1670	-0.0723	-0.0800
7250	2.5	1.4904	0.0634	-0.1146	-0.0692
	3.0	1.4412	0.0941	-0.1038	-0.0875
7500	2.5	1.4364	-0.0029	-0.1437	-0.0725
	3.0	1.4047	0.0231	-0.1329	-0.0927
7750	2.5	1.3772	-0.0605	-0.1694	-0.0750
	3.0	1.3630	-0.0370	-0.1595	-0.0969
8000	2.5	1.3143	-0.1111	-0.1919	-0.0775
	3.0	1.3150	-0.0884	-0.1830	-0.1009
8250	2.5	1.2438	-0.1532	-0.2101	-0.0812
	3.0	1.2595	-0.1332	-0.2028	-0.1044
8500	2.5	1.1690	-0.1885	-0.2254	-0.0845
	3.0	1.1945	-0.1709	-0.2190	-0.1074
8750	2.5	1.0928	-0.2164	-0.2379	-0.0889
	3.0	1.1284	-0.2032	-0.2331	-0.1111
9000	2.5	1.0181	-0.2374	-0.2477	-0.0948
	3.0	1.0604	-0.2293	-0.2447	-0.1150
9250	2.5	0.9465	-0.2529	-0.2551	-0.1019
	3.0	0.9932	-0.2499	-0.2538	-0.1190
9500	2.5	0.8783	-0.2641	-0.2606	-0.1104
	3.0	0.9299	-0.2656	-0.2613	-0.1245
9750	2.5	0.8134	-0.2728	-0.2651	-0.1199
	3.0	0.8701	-0.2775	-0.2675	-0.1311
10000	2.5	0.7501	-0.2796	-0.2685	-0.1298
	3.0	0.8116	-0.2869	-0.2724	-0.1384
10500	2.5	0.6313	-0.2911	-0.2739	-0.1490
	3.0	0.6995	-0.3011	-0.2798	-0.1541
11000	2.5	0.5265	-0.3015	-0.2787	-0.1658
	3.0	0.5955	-0.3121	-0.2853	-0.1696
11500	3.0	0.5033	-0.3221	-0.2901	-0.1835
12000	3.0	0.4241	-0.3318	-0.2950	-0.1953
12500	3.0	0.3562	-0.3411	-0.3001	-0.2056
13000	3.0	0.2970	-0.3502	-0.3052	-0.2148
14000	3.0	0.1950	-0.3664	-0.3152	-0.2308
15000	3.0	0.1082	-0.3806	-0.3245	-0.2443
16000	3.0	0.0324	-0.3928	-0.3332	-0.2561
17000	3.0	-0.0353	-0.4032	-0.3414	-0.2667
18000	3.0	-0.0980	-0.4113	-0.3484	-0.2765
19000	3.0	-0.1569	-0.4168	-0.3537	-0.2856
20000	3.0	-0.2114	-0.4205	-0.3568	-0.2935
21000	3.0	-0.2588	-0.4241	-0.3590	-0.2999

TABLE 11

SYNTHESIZED  $u'g'r'i'z'$  COLORS FOR STELLAR MODEL ATMOSPHERES WITH  
[M/H] = -1.0,  $\log g \in \{2.5, 3.0\}$ 

$T_{\text{eff}}$ (K)	$\log g$	$u' - g'$	$g' - r'$	$r' - i'$	$i' - z'$
3500	2.5	3.3182	1.4437	0.6723	0.4892
	3.0	3.1877	1.4408	0.6611	0.4555
3750	2.5	3.1097	1.2859	0.5429	0.3559
	3.0	3.0120	1.2992	0.5543	0.3487
4000	2.5	2.7206	1.0853	0.4501	0.2698
	3.0	2.6921	1.0997	0.4504	0.2692
4250	2.5	2.3605	0.9141	0.3769	0.2180
	3.0	2.3301	0.9188	0.3763	0.2159
4500	2.5	2.0644	0.7901	0.3173	0.1758
	3.0	2.0342	0.7857	0.3165	0.1741
4750	2.5	1.8028	0.6940	0.2692	0.1377
	3.0	1.7764	0.6868	0.2677	0.1369
5000	2.5	1.5806	0.6094	0.2289	0.1041
	3.0	1.5522	0.6034	0.2275	0.1041
5250	2.5	1.4033	0.5300	0.1920	0.0751
	3.0	1.3712	0.5274	0.1911	0.0752
5500	2.5	1.2754	0.4531	0.1567	0.0502
	3.0	1.2357	0.4543	0.1574	0.0501
5750	2.5	1.1950	0.3808	0.1224	0.0281
	3.0	1.1447	0.3853	0.1247	0.0278
6000	2.5	1.1499	0.3145	0.0885	0.0087
	3.0	1.0912	0.3212	0.0927	0.0078
6250	2.5	1.1285	0.2521	0.0552	-0.0079
	3.0	1.0644	0.2621	0.0609	-0.0104
6500	2.5	1.1216	0.1935	0.0222	-0.0218
	3.0	1.0560	0.2062	0.0296	-0.0263
6750	2.5	1.2055	0.0921	-0.0276	-0.0311
	3.0	1.0600	0.1521	-0.0014	-0.0400
7000	2.5	1.2276	0.0340	-0.0617	-0.0389
	3.0	1.1530	0.0593	-0.0481	-0.0508
7250	2.5	1.2463	-0.0237	-0.0943	-0.0442
	3.0	1.1796	0.0065	-0.0804	-0.0597
7500	2.5	1.2565	-0.0824	-0.1237	-0.0475
	3.0	1.2023	-0.0466	-0.1112	-0.0663
7750	2.5	1.2489	-0.1299	-0.1507	-0.0504
	3.0	1.2146	-0.0995	-0.1381	-0.0709
8000	2.5	1.2214	-0.1667	-0.1739	-0.0531
	3.0	1.2092	-0.1434	-0.1625	-0.0747
8250	2.5	1.1791	-0.1956	-0.1928	-0.0568
	3.0	1.1860	-0.1764	-0.1836	-0.0788
8500	2.5	1.1272	-0.2181	-0.2076	-0.0618
	3.0	1.1496	-0.2034	-0.2007	-0.0829
8750	2.5	1.0657	-0.2347	-0.2187	-0.0672
	3.0	1.1024	-0.2247	-0.2144	-0.0873
9000	2.5	1.0008	-0.2453	-0.2270	-0.0744
	3.0	1.0479	-0.2403	-0.2248	-0.0929
9250	2.5	0.9377	-0.2535	-0.2335	-0.0824
	3.0	0.9911	-0.2528	-0.2332	-0.0988
9500	2.5	0.8760	-0.2598	-0.2383	-0.0908
	3.0	0.9323	-0.2625	-0.2396	-0.1044
9750	2.5	0.8189	-0.2650	-0.2424	-0.0996
	3.0	0.8761	-0.2701	-0.2450	-0.1108
10000	2.5	0.7667	-0.2697	-0.2463	-0.1086
	3.0	0.8242	-0.2765	-0.2497	-0.1177
10500	2.5	0.6725	-0.2784	-0.2534	-0.1258
	3.0	0.7305	-0.2873	-0.2576	-0.1317
11000	2.5	0.5893	-0.2868	-0.2598	-0.1414
	3.0	0.6477	-0.2965	-0.2646	-0.1456
11500	2.5	0.5151	-0.2950	-0.2658	-0.1552
	3.0	0.5734	-0.3050	-0.2709	-0.1584
12000	2.5	0.4489	-0.3031	-0.2715	-0.1673
	3.0	0.5067	-0.3133	-0.2766	-0.1701
12500	2.5	0.3897	-0.3110	-0.2771	-0.1782
	3.0	0.4465	-0.3213	-0.2820	-0.1805
13000	2.5	0.3363	-0.3189	-0.2824	-0.1879
	3.0	0.3923	-0.3291	-0.2872	-0.1899
14000	2.5	0.2421	-0.3336	-0.2927	-0.2050
	3.0	0.2982	-0.3441	-0.2972	-0.2063
15000	2.5	0.1593	-0.3470	-0.3020	-0.2198
	3.0	0.2175	-0.3580	-0.3065	-0.2204

NOTE.—Colors were synthesized using spectra from Kurucz 1991.

TABLE 11—*Continued*

$T_{\text{eff}}$ (K)	$\log g$	$u' - g'$	$g' - r'$	$r' - i'$	$i' - z'$
16000.....	2.5	0.0838	-0.3589	-0.3105	-0.2329
	3.0	0.1456	-0.3707	-0.3152	-0.2327
17000.....	2.5	0.0138	-0.3693	-0.3179	-0.2446
	3.0	0.0801	-0.3824	-0.3230	-0.2438
18000.....	2.5	-0.0514	-0.3781	-0.3244	-0.2553
	3.0	0.0195	-0.3929	-0.3302	-0.2538
19000.....	2.5	-0.1122	-0.3851	-0.3300	-0.2650
	3.0	-0.0360	-0.4025	-0.3366	-0.2629
20000.....	3.0	-0.0869	-0.4111	-0.3427	-0.2712
21000.....	3.0	-0.1340	-0.4188	-0.3482	-0.2788
22000.....	3.0	-0.1780	-0.4257	-0.3529	-0.2858
23000.....	3.0	-0.2189	-0.4320	-0.3572	-0.2922
24000.....	3.0	-0.2566	-0.4386	-0.3618	-0.2981
25000.....	3.0	-0.2933	-0.4447	-0.3664	-0.3040
26000.....	3.0	-0.3316	-0.4479	-0.3694	-0.3095

NOTE.—Colors were synthesized using spectra from Kurucz 1991.

Cayrel de Strobel et al. (1997) list  $[\text{Fe}/\text{H}]$  values for 37 of the GS stars; of these, nine fall in the range  $0.5 < g' - r' < 0.8$ , and we show them as diamonds in Figure 8. If more than one metallicity is given, we plot all the reported values. The data are in rough agreement with the models, except for one outlier at  $l = -0.245$ . Unfortunately, these data only test the high-metallicity region of the distribution.

We note that there will be some overlap of the distribution in Figure 8 with white dwarfs, unusual stars, and non-stellar objects; the extent of such overlap must eventually be determined observationally. However, Figure 8 can provide valuable guidance for photometric analysis of the large quantities of stellar data that the SDSS will produce. For example, such information might be used to identify objects tentatively with  $l > 0.19$  as very low metallicity stars and tag them for follow-up.

If one were to exclude the  $r' - i'$  color from consideration (using  $\hat{l} = [-0.533, 0.846, 0.0]$ ), then the resulting distribution of  $[\text{M}/\text{H}]$  versus  $(r - r_0) \cdot (\hat{l})$  has more than twice the width of the distribution in Figure 8. This increase in width degrades the accuracy with which metallicities can be assigned; in particular, the high-metallicity dwarfs and  $[\text{M}/\text{H}] = -1$  giants overlap in  $(r - r_0) \cdot (\hat{l})$ . It is critical for this method of metallicity estimation that photometry be obtained in all four  $u'g'r'i'$  filters.

## 6. PHOTOMETRIC SURFACE GRAVITY SEPARATION FOR A STARS

Inspection of Figures 3 and 7 suggests that stars in the range  $-0.15 < g' - r' < 0.00$  (corresponding roughly to A stars) can be well separated by surface gravity using the  $u' - g'$ ,  $g' - r'$ ,  $r' - i'$ , and  $i' - z'$  colors. To find the optimal direction for separating A stars by gravity, we estimate the gradients of  $\log g$ ,  $T$ , and  $[\text{M}/\text{H}]$  in this region; we seek multicolor components that maximize the change in  $\log g$  while minimizing the changes in  $T$  and  $[\text{M}/\text{H}]$ .

We use the color of the model star with  $\log g = 3$ ,  $[\text{M}/\text{H}] = -1$ , and  $T = 7750$  K as a reference point. We estimate the direction of local surface gravity gradient by comparing the colors of that star with the colors of the model with  $\log g = 4$ ,  $[\text{M}/\text{H}] = -1$ , and  $T = 7750$ . The directions of the temperature and metallicity gradients for A stars are estimated in a similar manner. The gradient unit

TABLE 12

SYNTHESIZED  $u'g'r'i'z'$  COLORS FOR STELLAR MODEL ATMOSPHERES WITH  $[\text{M}/\text{H}] = -2.0$ ,  $\log g \in \{2.5, 3.0\}$

$T_{\text{eff}}$ (K)	$\log g$	$u' - g'$	$g' - r'$	$r' - i'$	$i' - z'$
3500.....	2.5	3.1110	1.4609	0.6665	0.3886
	3.0	3.0548	1.4607	0.6616	0.3830
3750.....	2.5	2.8167	1.2447	0.5619	0.3258
	3.0	2.7232	1.2400	0.5616	0.3190
4000.....	2.5	2.4577	1.0336	0.4597	0.2664
	3.0	2.4087	1.0379	0.4637	0.2648
4250.....	2.5	2.1117	0.8812	0.3896	0.2173
	3.0	2.0762	0.8732	0.3853	0.2155
4500.....	2.5	1.8103	0.7718	0.3345	0.1754
	3.0	1.7777	0.7599	0.3305	0.1742
4750.....	2.5	1.5494	0.6761	0.2880	0.1398
	3.0	1.5221	0.6678	0.2849	0.1389
5000.....	2.5	1.3482	0.5860	0.2446	0.1090
	3.0	1.3158	0.5804	0.2426	0.1086
5250.....	2.5	1.2052	0.4999	0.2027	0.0818
	3.0	1.1693	0.5021	0.2038	0.0818
5500.....	2.5	1.1170	0.4252	0.1643	0.0572
	3.0	1.0710	0.4285	0.1664	0.0575
5750.....	2.5	1.0678	0.3587	0.1288	0.0348
	3.0	1.0131	0.3642	0.1319	0.0350
6000.....	2.5	1.0465	0.2968	0.0950	0.0147
	3.0	0.9849	0.3052	0.0994	0.0144
6250.....	2.5	1.0436	0.2379	0.0618	-0.0027
	3.0	0.9769	0.2492	0.0676	-0.0044
6500.....	2.5	1.0521	0.1818	0.0293	-0.0178
	3.0	0.9840	0.1958	0.0365	-0.0210
6750.....	2.5	1.1458	0.0810	-0.0203	-0.0270
	3.0	1.0012	0.1435	0.0058	-0.0358
7000.....	2.5	1.1810	0.0252	-0.0550	-0.0352
	3.0	1.1017	0.0518	-0.0407	-0.0463
7250.....	2.5	1.2109	-0.0305	-0.0885	-0.0408
	3.0	1.1404	0.0004	-0.0737	-0.0557
7500.....	2.5	1.2303	-0.0875	-0.1185	-0.0442
	3.0	1.1727	-0.0511	-0.1051	-0.0627
7750.....	2.5	1.2306	-0.1343	-0.1458	-0.0470
	3.0	1.1934	-0.1021	-0.1329	-0.0674
8000.....	2.5	1.2096	-0.1696	-0.1696	-0.0498
	3.0	1.1952	-0.1456	-0.1575	-0.0713
8250.....	2.5	1.1710	-0.1965	-0.1888	-0.0538
	3.0	1.1771	-0.1774	-0.1792	-0.0757
8500.....	2.5	1.1202	-0.2172	-0.2038	-0.0591
	3.0	1.1440	-0.2029	-0.1969	-0.0801
8750.....	2.5	1.0576	-0.2320	-0.2145	-0.0649
	3.0	1.0966	-0.2229	-0.2105	-0.0846
9000.....	2.5	0.9937	-0.2424	-0.2227	-0.0720
	3.0	1.0429	-0.2381	-0.2211	-0.0902
9250.....	2.5	0.9327	-0.2498	-0.2290	-0.0801
	3.0	0.9869	-0.2496	-0.2293	-0.0960
9500.....	2.5	0.8752	-0.2559	-0.2339	-0.0882
	3.0	0.9310	-0.2588	-0.2356	-0.1017
9750.....	2.5	0.8223	-0.2612	-0.2383	-0.0966
	3.0	0.8789	-0.2663	-0.2409	-0.1080
10000.....	2.5	0.7734	-0.2660	-0.2424	-0.1052
	3.0	0.8303	-0.2727	-0.2458	-0.1146
10500.....	2.5	0.6851	-0.2753	-0.2499	-0.1216
	3.0	0.7419	-0.2837	-0.2541	-0.1282
11000.....	2.5	0.6067	-0.2843	-0.2568	-0.1367
	3.0	0.6633	-0.2934	-0.2614	-0.1415
11500.....	2.5	0.5362	-0.2929	-0.2633	-0.1501
	3.0	0.5927	-0.3025	-0.2680	-0.1540
12000.....	2.5	0.4725	-0.3013	-0.2694	-0.1623
	3.0	0.5288	-0.3111	-0.2741	-0.1654
12500.....	2.5	0.4147	-0.3095	-0.2753	-0.1731
	3.0	0.4707	-0.3194	-0.2800	-0.1757
13000.....	2.5	0.3618	-0.3175	-0.2808	-0.1830
	3.0	0.4176	-0.3275	-0.2854	-0.1852
14000.....	2.5	0.2673	-0.3324	-0.2913	-0.2005
	3.0	0.3236	-0.3427	-0.2958	-0.2019
15000.....	2.5	0.1833	-0.3456	-0.3008	-0.2157
	3.0	0.2418	-0.3566	-0.3054	-0.2163

TABLE 12—Continuum

$T_{\text{eff}}$ (K)	$\log g$	$u' - g'$	$g' - r'$	$r' - i'$	$i' - z'$
16000.....	2.5	0.1068	-0.3572	-0.3092	-0.2291
	3.0	0.1686	-0.3693	-0.3141	-0.2291
17000.....	2.5	0.0362	-0.3674	-0.3164	-0.2411
	3.0	0.1017	-0.3807	-0.3218	-0.2406
18000.....	2.5	-0.0289	-0.3764	-0.3227	-0.2519
	3.0	0.0402	-0.3910	-0.3288	-0.2508
19000.....	2.5	-0.0881	-0.3844	-0.3286	-0.2615
	3.0	-0.0162	-0.4005	-0.3350	-0.2599
20000.....	3.0	-0.0668	-0.4095	-0.3409	-0.2683
21000.....	3.0	-0.1129	-0.4179	-0.3466	-0.2759
22000.....	3.0	-0.1554	-0.4259	-0.3519	-0.2830
23000.....	3.0	-0.1954	-0.4334	-0.3572	-0.2895
24000.....	3.0	-0.2338	-0.4407	-0.3621	-0.2959
25000.....	3.0	-0.2726	-0.4471	-0.3672	-0.3021
26000.....	3.0	-0.3148	-0.4504	-0.3704	-0.3082

NOTE.—Colors were synthesized using spectra from Kurucz 1991.

vectors are

$$\hat{g} \equiv \frac{\nabla \log g}{\|\nabla \log g\|} = -0.875\hat{x}_{u'-g'} + 0.409\hat{x}_{g'-r'} + 0.182\hat{x}_{r'-i'} - 0.186\hat{x}_{i'-z'}, \quad (4)$$

$$\hat{T} \equiv \frac{\nabla T}{\|\nabla T\|} = -0.107\hat{x}_{u'-g'} - 0.867\hat{x}_{g'-r'} - 0.482\hat{x}_{r'-i'} - 0.075\hat{x}_{i'-z'}, \quad (5)$$

$$\hat{M} \equiv \frac{\nabla[M/H]}{\|\nabla[M/H]\|} = 0.952\hat{x}_{u'-g'} + 0.117\hat{x}_{g'-r'} - 0.234\hat{x}_{r'-i'} - 0.157\hat{x}_{i'-z'}, \quad (6)$$

where  $\hat{x}_{y-z}$  is a unit vector in the direction of variation in the  $y-z$  color. We are seeking a unit vector that is perpendicular to  $\hat{T}$  and  $\hat{M}$  and is as closely aligned with  $\hat{g}$  as possible. In order to find this vector, we first solve for the unit vector,  $\hat{N}$ , which is normal to  $\hat{g}$ ,  $\hat{T}$ , and  $\hat{M}$ :

$$\hat{N} = -0.112\hat{x}_{u'-g'} + 0.348\hat{x}_{g'-r'} - 0.697\hat{x}_{r'-i'} + 0.616\hat{x}_{i'-z'}; \quad (7)$$

$\hat{N}$  lies in the direction of least variation in  $\log g$ ,  $T$ , and  $[M/H]$ .

To find the optimal direction for color separation by surface gravity, we then construct the vector which is perpendicular to  $\hat{T}$ ,  $\hat{M}$ , and  $\hat{N}$ :

$$\hat{v} = 0.283\hat{x}_{u'-g'} - 0.354\hat{x}_{g'-r'} + 0.455\hat{x}_{r'-i'} + 0.766\hat{x}_{i'-z'}. \quad (8)$$

Figure 9 shows the separation by gravity along this unit vector. There is a tight correlation for  $-0.15 < g' - r' < 0.00$ , with a looser correlation if the  $g' - r'$  range is extended to  $-0.20 < g' - r' < 0.25$ . Accurate measurements of other stellar properties allow better constraint of  $\log g$ ; for example, metallicity measurement would result in a tighter limit on the value of  $\log g$ . This relation, of course, applies to unreddened or dereddened stars only.

Eight of the GS stars have  $-0.15 < g' - r' < 0.00$ ; five of these have spectroscopic luminosity classes listed in Table 2. The values of  $r' - i'$  and luminosity classes for these stars are: 0.219 (?), 0.220 (V), 0.226 (III), 0.232 (?), 0.237 (?), 0.238 (IV),

TABLE 13

SYNTHESIZED  $u'g'r'i'z'$  COLORS FOR STELLAR MODEL ATMOSPHERES WITH  $[M/H] = -5.0$ ,  $\log g \in \{2.5, 3.0\}$

$T_{\text{eff}}$ (K)	$\log g$	$u' - g'$	$g' - r'$	$r' - i'$	$i' - z'$
3500.....	2.5	3.4620	1.7048	0.8347	0.4482
	3.0	3.4815	1.7135	0.8274	0.4455
3750.....	2.5	2.8162	1.3461	0.6435	0.3414
	3.0	2.8097	1.3350	0.6358	0.3383
4000.....	2.5	2.3087	1.1028	0.5242	0.2762
	3.0	2.2209	1.0753	0.5140	0.2704
4250.....	2.5	1.9103	0.9216	0.4353	0.2266
	3.0	1.8216	0.8974	0.4291	0.2230
4500.....	2.5	1.5804	0.7719	0.3621	0.1834
	3.0	1.5247	0.7597	0.3594	0.1824
4750.....	2.5	1.3442	0.6562	0.3026	0.1471
	3.0	1.2993	0.6494	0.3017	0.1467
5000.....	2.5	1.1822	0.5623	0.2529	0.1153
	3.0	1.1415	0.5607	0.2535	0.1154
5250.....	2.5	1.0771	0.4820	0.2090	0.0874
	3.0	1.0342	0.4831	0.2107	0.0878
5500.....	2.5	1.0151	0.4129	0.1693	0.0622
	3.0	0.9671	0.4166	0.1722	0.0628
5750.....	2.5	0.9849	0.3508	0.1329	0.0392
	3.0	0.9300	0.3564	0.1366	0.0397
6000.....	2.5	0.9780	0.2918	0.0985	0.0187
	3.0	0.9165	0.3007	0.1034	0.0185
6250.....	2.5	0.9879	0.2345	0.0655	0.0007
	3.0	0.9207	0.2466	0.0717	-0.0007
6500.....	2.5	1.0082	0.1797	0.0330	-0.0146
	3.0	0.9385	0.1945	0.0403	-0.0178
6750.....	2.5	1.0440	0.1199	-0.0014	-0.0266
	3.0	0.9639	0.1432	0.0097	-0.0328
7000.....	2.5	1.1534	0.0245	-0.0509	-0.0330
	3.0	1.0030	0.0882	-0.0228	-0.0452
7250.....	2.5	1.1910	-0.0309	-0.0849	-0.0388
	3.0	1.1179	0.0005	-0.0697	-0.0534
7500.....	2.5	1.2157	-0.0867	-0.1155	-0.0422
	3.0	1.1562	-0.0499	-0.1016	-0.0606
7750.....	2.5	1.2208	-0.1338	-0.1431	-0.0453
	3.0	1.1820	-0.1004	-0.1301	-0.0656
8000.....	2.5	1.2028	-0.1681	-0.1674	-0.0482
	3.0	1.1878	-0.1441	-0.1549	-0.0697
8250.....	2.5	1.1669	-0.1953	-0.1869	-0.0521
	3.0	1.1727	-0.1760	-0.1770	-0.0741
8500.....	2.5	1.1173	-0.2155	-0.2019	-0.0576
	3.0	1.1416	-0.2013	-0.1949	-0.0787
8750.....	2.5	1.0565	-0.2299	-0.2126	-0.0635
	3.0	1.0961	-0.2212	-0.2086	-0.0832
9000.....	2.5	0.9949	-0.2400	-0.2208	-0.0707
	3.0	1.0445	-0.2362	-0.2193	-0.0888
9250.....	2.5	0.9355	-0.2475	-0.2270	-0.0787
	3.0	0.9906	-0.2476	-0.2276	-0.0946
9500.....	2.5	0.8793	-0.2537	-0.2319	-0.0867
	3.0	0.9363	-0.2567	-0.2339	-0.1004
9750.....	2.5	0.8277	-0.2590	-0.2364	-0.0950
	3.0	0.8849	-0.2641	-0.2394	-0.1066
10000.....	2.5	0.7799	-0.2641	-0.2404	-0.1033
	3.0	0.8367	-0.2706	-0.2441	-0.1131
10500.....	2.5	0.6946	-0.2738	-0.2483	-0.1193
	3.0	0.7501	-0.2819	-0.2525	-0.1263
11000.....	2.5	0.6192	-0.2832	-0.2555	-0.1339
	3.0	0.6738	-0.2920	-0.2600	-0.1393
11500.....	2.5	0.5514	-0.2923	-0.2624	-0.1471
	3.0	0.6056	-0.3015	-0.2669	-0.1515
12000.....	2.5	0.4895	-0.3011	-0.2688	-0.1591
	3.0	0.5438	-0.3105	-0.2734	-0.1627
12500.....	2.5	0.4325	-0.3095	-0.2749	-0.1700
	3.0	0.4870	-0.3191	-0.2794	-0.1731
13000.....	2.5	0.3797	-0.3176	-0.2806	-0.1800
	3.0	0.4345	-0.3273	-0.2852	-0.1825
14000.....	2.5	0.2840	-0.3323	-0.2913	-0.1978
	3.0	0.3402	-0.3427	-0.2958	-0.1995
15000.....	2.5	0.1987	-0.3454	-0.3007	-0.2133
	3.0	0.2571	-0.3566	-0.3053	-0.2142



TABLE 13—Continued

$T_{\text{eff}}$ (K)	$\log g$	$u' - g'$	$g' - r'$	$r' - i'$	$i' - z'$
16000.....	2.5	0.1211	-0.3568	-0.3090	-0.2270
	3.0	0.1825	-0.3692	-0.3139	-0.2273
17000.....	2.5	0.0501	-0.3668	-0.3161	-0.2391
	3.0	0.1146	-0.3803	-0.3216	-0.2389
18000.....	2.5	-0.0147	-0.3758	-0.3224	-0.2499
	3.0	0.0524	-0.3904	-0.3285	-0.2493
19000.....	2.5	-0.0731	-0.3844	-0.3282	-0.2595
	3.0	-0.0041	-0.3998	-0.3346	-0.2585
20000.....	3.0	-0.0545	-0.4089	-0.3406	-0.2667
21000.....	3.0	-0.0998	-0.4178	-0.3464	-0.2743
22000.....	3.0	-0.1411	-0.4264	-0.3521	-0.2814
23000.....	3.0	-0.1802	-0.4349	-0.3579	-0.2882
24000.....	3.0	-0.2186	-0.4430	-0.3636	-0.2948
25000.....	3.0	-0.2589	-0.4498	-0.3691	-0.3016
26000.....	3.0	-0.3053	-0.4524	-0.3720	-0.3081

NOTE.—Colors were synthesized using spectra from Kurucz 1991.

0.251 (IV), and 0.293 (V). These data suggest that there is not much difference between the surface gravities of A stars with different luminosity classes. In fact, the outlier with the lowest computed surface gravity ( $\log g \sim 2.3$ ) is classified as

TABLE 14

SYNTHESIZED  $u'g'r'i'z'$  COLORS FOR STELLAR MODEL ATMOSPHERES WITH  $[M/H] = -1.0$ ,  $\log g \in \{1.0, 1.5, 2.0\}$

$T_{\text{eff}}$ (K)	$\log g$	$u' - g'$	$g' - r'$	$r' - i'$	$i' - z'$
4000.....	1.0	3.1271	1.1253	0.4627	0.2803
	1.5	2.9310	1.0955	0.4561	0.2752
	2.0	2.7966	1.0831	0.4522	0.2718
4250.....	1.0	2.7304	0.9761	0.3871	0.2281
	1.5	2.5593	0.9409	0.3815	0.2240
	2.0	2.4365	0.9210	0.3783	0.2206
4500.....	1.0	2.3697	0.8596	0.3295	0.1808
	1.5	2.2303	0.8250	0.3223	0.1790
	2.0	2.1280	0.8016	0.3184	0.1773
4750.....	1.0	2.0548	0.7534	0.2827	0.1388
	1.5	1.9417	0.7257	0.2757	0.1387
	2.0	1.8571	0.7064	0.2712	0.1386
5000.....	1.0	1.7990	0.6481	0.2379	0.1036
	1.5	1.7033	0.6308	0.2336	0.1036
	2.0	1.6298	0.6184	0.2309	0.1038
5250.....	1.0	1.6092	0.5460	0.1942	0.0755
	1.5	1.5214	0.5389	0.1931	0.0751
	2.0	1.4524	0.5335	0.1926	0.0749
5500.....	1.0	1.4840	0.4531	0.1522	0.0522
	1.5	1.4006	0.4514	0.1541	0.0508
	2.0	1.3309	0.4518	0.1557	0.0503
5750.....	1.0	1.4055	0.3695	0.1117	0.0342
	1.5	1.3290	0.3721	0.1156	0.0309
	2.0	1.2568	0.3760	0.1194	0.0289
6000.....	1.0	1.4145	0.2458	0.0556	0.0254
	1.5	1.2840	0.2995	0.0782	0.0150
	2.0	1.2163	0.3066	0.0836	0.0110
6250.....	1.0	1.3948	0.1671	0.0151	0.0185
	1.5	1.3269	0.1835	0.0241	0.0069
	2.0	1.1945	0.2416	0.0484	-0.0035
6500.....	1.0	1.3822	0.0899	-0.0241	0.0157
	1.5	1.3288	0.1127	-0.0142	0.0002
	2.0	1.2615	0.1327	-0.0037	-0.0118
6750.....	1.0	1.3666	0.0128	-0.0607	0.0158
	1.5	1.3311	0.0430	-0.0509	-0.0030
	2.0	1.2753	0.0688	-0.0397	-0.0189
7000.....	1.0	1.3414	-0.0511	-0.0951	0.0167
	1.5	1.3286	-0.0274	-0.0850	-0.0037
	2.0	1.2884	0.0054	-0.0746	-0.0228

NOTE.—Colors were synthesized using spectra from Kurucz 1991.

TABLE 15

SYNTHESIZED  $u'g'r'i'z'$  COLORS FOR STELLAR MODEL ATMOSPHERES WITH  $[M/H] = 0.0$ ,  $\log g = 5.0$

$T_{\text{eff}}$ (K)	$\log g$	$u' - g'$	$g' - r'$	$r' - i'$	$i' - z'$
20000.....	5.0	-0.0135	-0.4176	-0.3463	-0.2909
21000.....	5.0	-0.0560	-0.4269	-0.3521	-0.2963
22000.....	5.0	-0.0951	-0.4357	-0.3579	-0.3015
23000.....	5.0	-0.1315	-0.4439	-0.3632	-0.3065
24000.....	5.0	-0.1659	-0.4514	-0.3685	-0.3113
25000.....	5.0	-0.1985	-0.4582	-0.3733	-0.3158
26000.....	5.0	-0.2291	-0.4645	-0.3777	-0.3200
27000.....	5.0	-0.2577	-0.4705	-0.3818	-0.3238
28000.....	5.0	-0.2839	-0.4764	-0.3858	-0.3275
29000.....	5.0	-0.3082	-0.4825	-0.3898	-0.3310
30000.....	5.0	-0.3309	-0.4885	-0.3938	-0.3343
31000.....	5.0	-0.3525	-0.4942	-0.3976	-0.3374
32000.....	5.0	-0.3727	-0.4993	-0.4009	-0.3401
33000.....	5.0	-0.3916	-0.5035	-0.4038	-0.3424
34000.....	5.0	-0.4087	-0.5070	-0.4061	-0.3444
35000.....	5.0	-0.4240	-0.5093	-0.4079	-0.3459
36000.....	5.0	-0.4372	-0.5107	-0.4092	-0.3468
37000.....	5.0	-0.4488	-0.5115	-0.4098	-0.3473
38000.....	5.0	-0.4585	-0.5119	-0.4101	-0.3473
39000.....	5.0	-0.4667	-0.5124	-0.4103	-0.3472
40000.....	5.0	-0.4735	-0.5132	-0.4107	-0.3471
41000.....	5.0	-0.4795	-0.5142	-0.4112	-0.3472
42000.....	5.0	-0.4847	-0.5155	-0.4119	-0.3474
43000.....	5.0	-0.4894	-0.5169	-0.4126	-0.3477
44000.....	5.0	-0.4938	-0.5182	-0.4134	-0.3481
45000.....	5.0	-0.4978	-0.5195	-0.4141	-0.3485
46000.....	5.0	-0.5016	-0.5208	-0.4147	-0.3489
47000.....	5.0	-0.5051	-0.5220	-0.4153	-0.3493
48000.....	5.0	-0.5085	-0.5231	-0.4158	-0.3496
49000.....	5.0	-0.5115	-0.5241	-0.4163	-0.3499
50000.....	5.0	-0.5145	-0.5251	-0.4167	-0.3502

NOTE.—Colors were synthesized using spectra from Kurucz 1991.

a dwarf. From Figure 9, we surmise that the other seven stars have surface gravities of  $2.7 < \log g < 3.7$ . The failure of photometric colors to distinguish between A giants and dwarfs by surface gravity is consistent with the findings of Newberg & Yanny (1998), who noticed that many A III stars appear on the main sequence in H-R diagrams of field stars with absolute magnitudes computed using parallaxes from the *Hipparcos* satellite. The measured range of surface gravities is somewhat lower than expected (see, e.g., Allen 1973, p. 213). Resolution of discrepancies among various determinations of  $\log g$  requires examination of determinations of  $\log g$  via, e.g., luminosity class and stellar modeling.

We note that only three of the 37 simulated white dwarfs in  $-0.20 < g-r < 0.25$  have  $r \cdot \hat{v} > 0.1$ , which suggests that white dwarfs and normal stars may be separated in this region of multicolor space. The discrimination of white dwarfs in a sample is dependent on good  $u'$ -band data; white dwarfs show the most separation from the normal star locus in  $u' - g'$  (Fig. 3a).

If fewer than four colors are available for a given data set, stars can still be separated by surface gravity, especially if  $u' - g'$  or  $i' - z'$  data are available. To find the direction that separates surface gravities for data with only  $g'r'i'z'$  data, for example, we find

$$\hat{v}_{g'r'i'z'} \equiv \frac{\hat{v} + 2.52\hat{N}}{\|\hat{v} + 2.52\hat{N}\|} = 0.193\hat{x}_{g'-r'} - 0.481\hat{x}_{r'-i'} + 0.855\hat{x}_{i'-z'}. \quad (9)$$

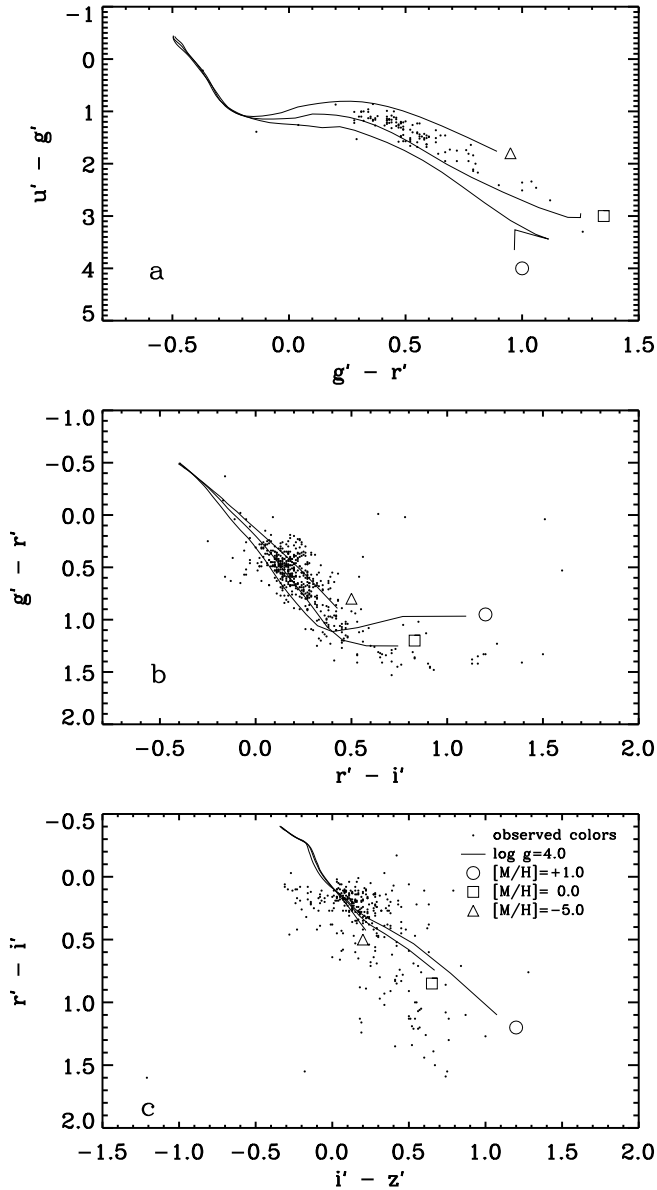


FIG. 6.—Comparison of observed colors (*dots*) for field objects of Richards et al. (1997) with synthetic colors for Kurucz model atmospheres for  $\log g = 4.0$ ,  $[M/H] = +1.0, 0.0, -5.0$  (solid curves labeled as in Fig. 3; Kurucz 1991). For simplicity, we denote all colors with superscript primes, although the observed colors are technically denoted with superscript asterisks (see § 4).

The correlation of this component with  $\log g$  is also high, but the separation by surface gravity is reduced by almost a factor of 3 compared with the four-dimensional solution. This follows from the fact that  $|\hat{v} \cdot \hat{g}| = 0.45$ , while  $|\hat{v}_{g'r'i'z'} \cdot \hat{g}| = 0.17$ . Similarly, one can construct  $\hat{v}_{u'g'r'i'}$ , which again produces a good correlation with  $\log g$ , but with  $|\hat{v}_{u'g'r'i'} \cdot \hat{g}| = 0.29$ .

## 7. CONCLUSIONS

We present synthetic  $u'g'r'i'z'$  photometry for Kurucz model stellar spectra and for white dwarf and Gunn-Stryker spectrophotometry. The synthetic colors of the models show qualitative agreement with the few published observations in these filters. Of the colors we study,  $u' - g'$  shows the most differentiation due to stellar properties; the  $g' - r'$ ,

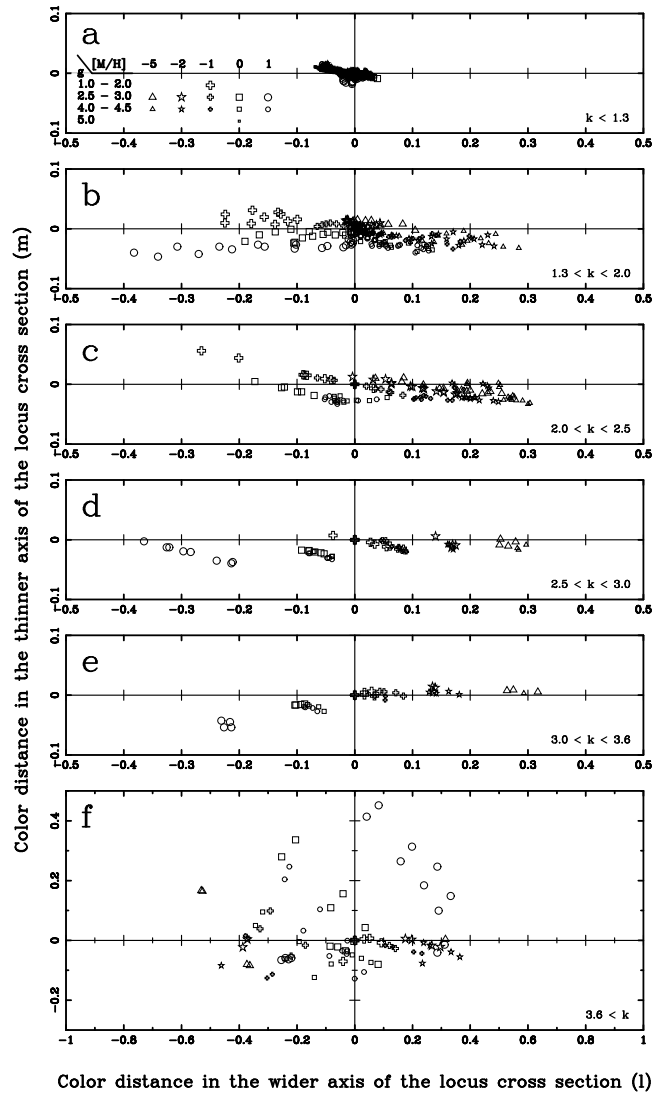


FIG. 7.—The locus of Kurucz model atmospheres (Kurucz 1991) as a function of the nonlinear principal color components  $k$ ,  $l$ , and  $m$ . The panels contain cross sections of the stellar locus from bluest (*a*) to reddest (*f*), labeled by  $k$  range. The values of  $k$  along the locus are given in Fig. 3. The symbol shapes indicate metallicity, and the symbol sizes indicate surface gravity as shown in the legend in the top panel. Note that the symbols separate roughly by size (surface gravity) in (*b*) and by shape (metallicity) in (*e*).

$r' - i'$ , and  $i' - z'$  colors show less dramatic separation. We demonstrate that synthetic  $u'g'r'i'z'$  photometry for modeled stars with a range of effective temperatures, surface gravities, and metallicities can provide guidance for photometrically locating stars with certain properties.

The synthetic colors indicate that white dwarfs and normal stars overlap in some color projections. Separation of white dwarfs and normal stars will be most successful using  $u' - g'$  data, since white dwarfs separate the most from normal stars in  $u' - g'$  versus  $g' - r'$ .

The synthetic colors of model atmospheres are consistent with those of Gunn-Stryker stellar spectra; the Gunn-Stryker colors lie mostly within the model stellar locus. The Gunn-Stryker colors include a “tail” of M stars not present in the model colors; since the modeling of such cool atmospheres contains known difficulties (i.e., molecular bands), some discrepancy is not surprising.

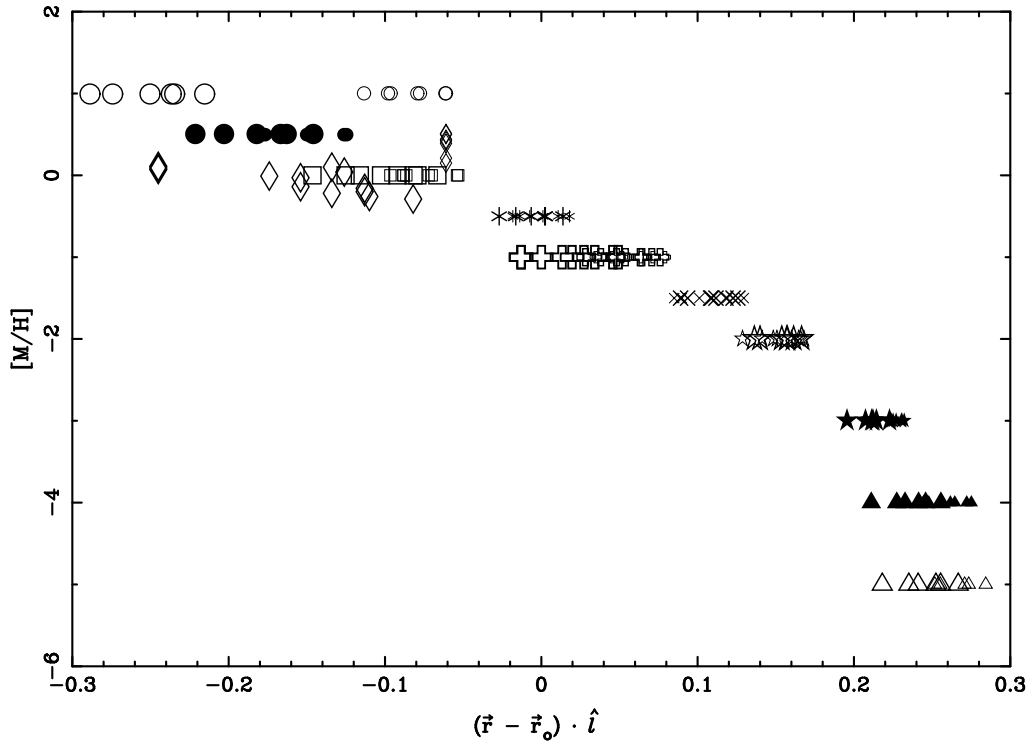


FIG. 8.—Metallicity separation as a function of  $(r - r_0) \cdot \hat{i} \cong l$  for Kurucz model atmospheres (Kurucz 1991) with  $0.5 < g' - r' < 0.8$ . Symbol sizes and shapes are as in Fig. 7; additional symbols are filled circles:  $[M/H] = +0.5$ , asterisks:  $[M/H] = -0.5$ , crosses:  $[M/H] = -1.5$ , filled stars:  $[M/H] = -3$ , and filled triangles:  $[M/H] = -4$ . The diamonds are (multiple) measurements of the metallicities of nine Gunn-Stryker stars from Cayrel de Strobel et al. (1997). Smaller diamonds are for a star with  $\log g \geq 3.5$ .

Because the stellar locus is basically two-dimensional through most of color space, it is not possible to separate stars simultaneously by temperature, metallicity, and surface gravity. There are, however, special cases in which

the locus shows color separation due to variation in a single stellar characteristic. In the range  $0.5 < g' - r' < 0.8$ , we use a parameterization of the stellar locus to determine the metallicities of stars to within about 0.5 dex. A star in the

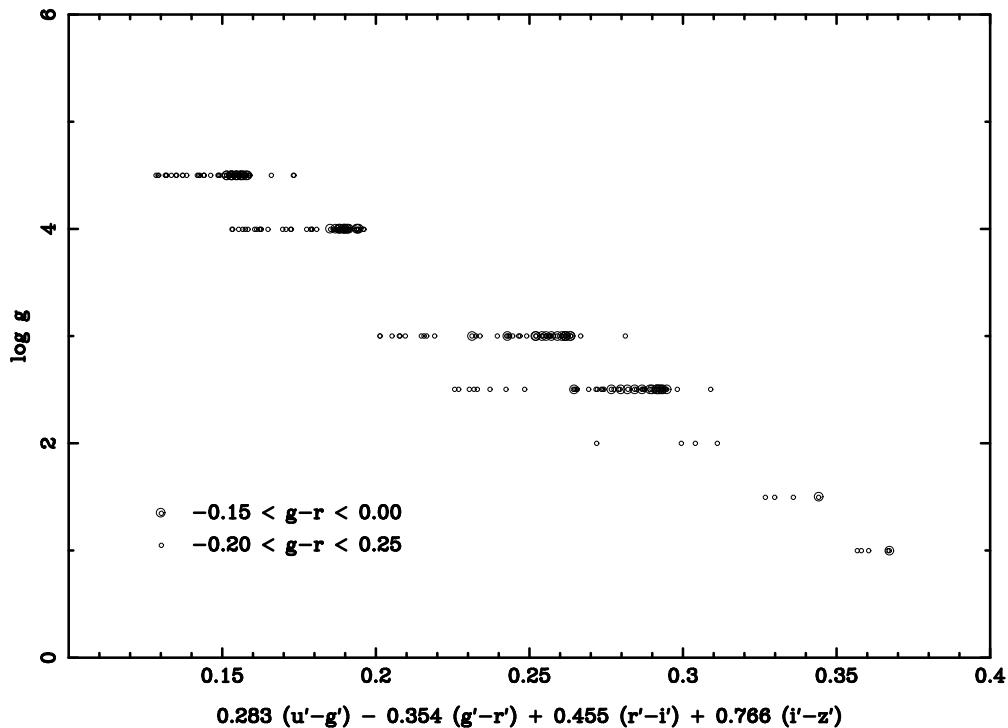


FIG. 9.—Surface gravity separation as a function of  $r \cdot \hat{v}$  (see § 6 for discussion) for Kurucz model atmospheres (Kurucz 1991) with  $-0.15 < g' - r' < 0.00$  (larger circles) and  $-0.20 < g' - r' < 0.25$  (smaller circles).

range  $18 \lesssim V \lesssim 20$ , near the limit of high-accuracy photometry in the SDSS, is either a G–K dwarf at 3–10 kpc, or a G giant at 30–80 kpc. Therefore we may assume that the vast majority of these stars are dwarfs and use our metallicity relationship to trace the metal abundance as a function of position in the Galactic halo. Other applications for photometric metallicity separation include tagging very low metallicity stars for spectroscopic follow-up.

In the range  $-0.15 < g' - r' < 0.00$ , we use unit vectors approximating the gradients in color space of metallicity, temperature, and surface gravity to develop a relation that best separates A stars by surface gravity. If the synthetic photometry is a reliable simulation of good photometric data, then it is possible to separate unreddened A stars by surface gravity and metallicity (Fig. 7*b*), though the metallicity separation for A stars is only a few percent in color space even for a large range of metallicities.

We have discovered discrepancies in several cases between synthetic colors of Gunn–Stryker stars, Kurucz model atmospheres, and external measurements of metallicities and surface gravities. These discrepancies could be explained by systematic error of  $\sim 5\%$  in the colors of either

the Gunn–Stryker stars or the Kurucz models, except at the very red end of the locus where the discrepancy is larger. Careful study of the various observational and theoretical data sets is required to resolve such discrepancy.

One can use techniques similar to those described above, along with the tables of synthetic photometry, to generate relations for other special cases. For example, if one had a sample of F stars that was known by other means to be dwarfs, then the two-dimensional locus could be used to determine the metallicity and temperature of the stars. Such algorithms can facilitate the analysis of large amounts of photometry that will be produced by surveys such as the SDSS.

The authors thank Fabio Favata, Masataka Fukugita, Jim Gunn, Bob Hindsley, Takashi Ichikawa, Richard Kron, Don Schneider, Kazu Shimasaku, and Brian Yanny for helpful comments, advice, and encouragement. We thank Robert Kurucz for providing his stellar model atmospheres. G. T. R. was supported in part by a fellowship from the Adler Planetarium. Electronic versions of Tables 2–15 may be obtained by contacting D. Lenz.

#### REFERENCES

- Allen, C. W. 1973, *Astrophysical Quantities* (London: Athlone)
- Bessell, M. S. 1990, *PASP*, 102, 1181
- Cayrel de Strobel, G., Soubiran, C., Friel, E. D., Ralite, N., & François, P. 1997, *A&AS*, 124, 299
- Fukugita, M., Ichikawa, T., Gunn, J. E., Doi, M., Shimasaku, K., & Schneider, D. P. 1996, *AJ*, 111, 1748 (F96)
- Green, R. F., Schmidt, M., & Liebert, J. 1986, *ApJS*, 61, 305
- Greenstein, J. L., & Liebert, J. W. 1990, *ApJ*, 360, 662
- Gunn, J. E. 1995, *BAAS*, 27, 875
- Gunn, J. E., & Knapp, G. R. 1993, in *ASP Conf. Proc. 43, Sky Surveys: Protostars to Protogalaxies*, ed. B. T. Soifer (San Francisco: ASP), 267
- Gunn, J. E., & Stryker, L. L. 1983, *ApJS*, 52, 121 (GS)
- Kent, S. M. 1994, *Ap&SS*, 217, 27
- Kurucz, R. L. 1979, *ApJS*, 40, 1
- . 1991, in *Precision Photometry: Astrophysics of the Galaxy*, ed. A. G. D. Philip, A. R. Uggren, & K. A. Janes (Schenectady: Davis), 27
- Mihalas, D. & Binney, J. 1981, *Galactic Astronomy* (2d ed.; New York: Freeman)
- Newberg, H. J., & Yanny, B. 1997, *ApJS*, 113, 89 (NY97)
- . 1998, *ApJ*, 499, L57
- Oke, J. B., & Gunn, J. E. 1983, *ApJ*, 266, 713 (OG)
- Richards, G. T., Yanny, B., Annis, J., Newberg, H. J. M., McKay, T. A., York, D. G., & Fan, X. 1997, *PASP*, 109, 39 (R97)